QUALITY OF SERVICE ANALYSIS FOR SLOTTED OPTICAL BURST SWITCHING NETWORKS

A THESIS

SUBMITTED TO THE DEPARTMENT OF ELECTRICAL AND

ELECTRONICS ENGINEERING

AND THE INSTITUTE OF ENGINEERING AND SCIENCES

OF BILKENT UNIVERSITY

IN PARTIAL FULFILLMENT OF THE REQUIREMENTS

FOR THE DEGREE OF

MASTER OF SCIENCE

By

Onur Öztürk

January 2008

I certify that I have read this thesis and that in my opinion it is fully adequate, in scope and in quality, as a thesis for the degree of Master of Science.

Assoc. Prof. Dr. Ezhan Karaşan(Supervisor)

I certify that I have read this thesis and that in my opinion it is fully adequate, in scope and in quality, as a thesis for the degree of Master of Science.

Assoc. Prof. Dr. Nail Akar

I certify that I have read this thesis and that in my opinion it is fully adequate, in scope and in quality, as a thesis for the degree of Master of Science.

Prof. Dr. Tuğrul Dayar

Approved for the Institute of Engineering and Sciences:

Prof. Dr. Mehmet Baray
Director of Institute of Engineering and Sciences

ABSTRACT

QUALITY OF SERVICE ANALYSIS FOR SLOTTED OPTICAL BURST SWITCHING NETWORKS

Onur Öztürk
M.S. in Electrical and Electronics Engineering
Supervisor: Assoc. Prof. Dr. Ezhan Karaşan
January 2008

Optical burst switching (OBS) is proposed as the switching paradigm of next-generation optical Internet. In OBS, IP packets from access networks are assembled into longer units of bursts allowing a lower level of switching granularity offered by the readily available optical technology. Although OBS was asynchronous in the earlier work, slotted OBS (SOBS) has recently caught the attention of the researchers due to performance gains achievable with synchronous infrastructures. In this thesis, we study the blocking probabilities in a slotted optical burst switching node fed with independent and identically distributed Poisson burst traffic and for which the burst sizes are a fixed integer multiple of the slot length. We develop a discrete time Markov chain based framework to obtain the blocking probabilities in systems with and without QoS differentiation. In particular, we study priority scheduling and offset-based QoS differentiation mechanisms for SOBS networks. The latter problem suffers from the curse of dimensionality, which we address by a discrete phase type approximation for the discrete Poisson distribution. The results obtained by using the moment-matched phase type distribution are shown to provide a very accurate approximation for the

blocking probabilities. Finally, we extend our framework to analyze the hybrid priority scheduling with unity-offset based differentiation scheme which proves to outperform the others in the degree of class isolation. We show that increasing burst length has an adverse affect on the attained QoS level. We also give a quantitative discussion of the trade off between the burst blocking probability and the slot granularity. As the slot duration is decreased, burst transmissions can be initiated in an earlier time decreasing the end-to-end delay in an SOBS network with a penalty of increased burst loss probability. We evaluate the burst blocking probabilities of a classless and two-class SOBS nodes as a function of the slot length, number of wavelengths and traffic load.

Keywords: Optical Burst Switching (OBS), Slotted Optical Burst Switching (SOBS), Quality of Service (QoS)

ÖZET

DİLİMLİ OPTİK ÇOĞUŞMA ANAHTARLAMALI AĞLARDA HİZMET NİTELİĞİ ÇÖZÜMLEMESİ

Onur Öztürk
Elektrik ve Elektronik Mühendisliği Bölümü Yüksek Lisans
Tez Yöneticisi: Doç. Dr. Ezhan Karaşan
Ocak 2008

Optik çoğuşma anahtarlaması (OBS), yeni nesil optik Internet anahtarlama paradigması olarak öne sürülmüştür. OBS'te erişim ağlarından gelen IP paketlerinin daha uzun çoğuşmalar şeklinde toplanması, hali hazırda bulunan optik teknolojinin sunduğu seviyede anahtarlama yapılmasına imkan sağlar. Öncül çalışmalarda OBS eşzamansız olmasına rağmen, eşzamanlı altyapılarla sağlanabilen başarım artışları nedeniyle dilimli OBS (SOBS) araştırmacıların dikkatini çekmiştir. Bu tezde, bağımsız ve özdeşçe dağılmış çoğuşma trafiğiyle beslenen ve çoğuşma uzunlukları dilim uzunluklarının sabit ve tam sayı katı olan bir SOBS düğümündeki çoğuşma kaybolma olasılıkları üzerine çalışıyoruz. Hizmet niteliği (QoS) ayrımı olan ve olmayan sistemlerdeki çoğuşma kaybolma olasılıklarını bulmak için ayrık zamanlı Markov zinciri tabanlı bir yapı geliştiriyoruz. SOBS ağlarda, özellikle öncelikli zaman çizelgelemesine ve kaydırmaya dayalı hizmet ayrımı mekanizmaları üzerine çalışıyoruz. İkinci problem, boyutları nedeniyle çözülmesi zor olduğundan, ayrık Poisson dağılımını PH tipi dağılımla yakınsıyoruz. Momentleri eşlenmiş PH tipi dağılımı kullanılarak elde edilen sonuçların, çoğuşma kaybolma olasılıklarına çok iyi bir

şekilde yakınsadığını gösteriyoruz. Son olarak, bu ayrık zamanlı Markov zinciri tabanlı yapıyı hem öncelikli zaman çizelgelemesine hem de kaydırmaya dayalı olan ve bu ikisine de sınıf izolasyonu derecesi bakımından üstün gelen melez bir hizmet ayrımı tekniğini çözümleyecek şekilde genişletiyoruz. Artan çoğuşma uzunluğunun ulaşılan hizmet niteliğine ters etki yaptığını gösteriyoruz. Ayrıca, dilim büyüklüğü ve çoğuşma kaybolma olasılığı arasındaki ödünleşimi niceliksel olarak tartışıyoruz. Dilim büyüklüğü azaldıkça artan çoğuşma kaybolma olasılığına karşın, çoğuşma iletimi daha erken bir zamanda başlatılarak uçtan uca gecikme azaltılabilir. Hizmet niteliği ayrımı olan ve olmayan SOBS ağlarda, çoğuşma uzunluğunun, dalgaboyu sayısının ve trafik yükünün fonksiyonu olarak çoğuşma kaybolma olasılıklarını hesaplıyoruz.

Anahtar Kelimeler: Optik Çoğuşma Anahtarlaması (OBS), Dilimli Optik Çoğuşma Anahtarlaması (SOBS), Hizmet Niteliği (QoS)

ACKNOWLEDGMENTS

I would like to thank Assoc. Prof. Dr. Ezhan Karaşan and Assoc. Prof. Dr. Nail Akar for their invaluable supervision and guidance throughout this thesis...

Hereby, I would also like to express my gratefulness to my family for giving me their restless support...

Contents

List of Figures

List of Tables

To my beloved Deniz ...

Chapter 1

Introduction

Optical burst switching (OBS), has been proposed as a viable transport architecture for next generation Internet with readily available technology [1], [2]. It is announced to be a versatile switching paradigm offering high network throughput with no mandatary optical buffering and processing. For that purpose, control and data planes are segregated by means of dedicated wavelengths. Since control packets are supposed to be much smaller than the transmitted data, assigning a single wavelength to the control plane has become a common practice. Packets arriving from different access networks are aggregated into so-called bursts at the edge of the OBS domain using one of the alternative burst assembly protocols [3]. Three types of nodes namely ingress, egress and core nodes exist in an OBS network. Ingress and egress nodes control the input and output traffic of the OBS network respectively, where core nodes manage the network traffic through the egress nodes. Based on its functionality, an OBS node may be all of them at the same time. Once a burst is formed at an ingress node, a burst control packet (BCP) is sent in advance out-of-band over the control channel in order to deliver the reservation request to intermediate core nodes. Each receiving node processes the BCP and forwards it to the downstream nodes if the

request can be fulfilled. If all nodes on the path from the source to the destination allocate necessary resources then the burst traverses the OBS network in a cut-through manner rather than the conventional store-and-forward way. At the egress node, IP packets inside the burst are extracted by a process called de-assembly by which they leave the optical domain. For the success of this operation, after sending the BCP, ingress node waits for an offset time equal to the total processing delay at the intermediate nodes before transmitting the bursts. Under just-enough-time (JET) reservation protocol, BCPs carry the burst and offset length information to the nodes so that resource allocation for bursts is done for only the burst transmission interval [1], [4].

Contention occurs in OBS when two or more bursts contend for the same output wavelength over overlapping time periods. Since one-way reservation protocol is used and there is no optical buffering in OBS, contention results in burst loss. Contention resolution have been so far one of the most challenging research topics among the OBS community due to high loss rates experienced by bursts. The most common technique for contention resolution is the wavelength conversion [5], [6], although other techniques such as fiber delay lines (FDLs) [7] or deflection routing [8] can be used as well. In this thesis, we assume that the OBS system employs only full wavelength conversion for which a burst can be switched onto any output wavelength towards its destination regardless of its original wavelength. Other schemes like partial or limited wavelength conversion are left out of the scope of this thesis [9]. If contention cannot be resolved by wavelength conversion, then all bursts other than a chosen one according to a predefined policy are dropped decreasing the throughput of the network. In OBS, no feedback mechanism is established to report such losses, hence retransmission of the packets inside these bursts are left to the upper layer protocols. This is in contrast with the electronically packet switched networks, where data in units of packets is received, stored and forwarded all electronically over shared links. The packet losses in these networks are prevented via buffering with a penalty

of increased queueing delay. It is thus very crucial to give a reduction in burst loss probabilities for the success of the OBS paradigm in next generation optical communications.

Like every communication system, OBS has both synchronous and asynchronous modes of operation and the choice between them has a significant impact on the loss probabilities. Most of the current OBS proposals are based on asynchronous operation in which bursts have variable sizes and are not aligned with the slot boundaries before entering the optical switch [10]. Implementation of asynchronous nodes is much simpler than their synchronous counterparts since no synchronization stage is needed [10]. On the other hand, partial overlap between two bursts due to timing uncertainty may result in loss of an entire burst. Therefore, asynchronous operation has an adverse effect on burst loss probabilities. Recently, there has been a surge of interest in synchronous (or slotted) optical burst switching (SOBS) systems due to the performance advantages of slotted operation [11], [12], [13]. SOBS is to OBS, what slotted ALOHA is to ALOHA and similar enhancements in relative performance for SOBS are already shown in [13]. In SOBS, data plane is divided into time slots of equal length and data bursts occupy either a single or a multiple number of slots in duration although most existing studies assume that the slot size and the burst length are the same in which case the system is also called SynOBS [12]. The control plane may also be divided into smaller slots in order to accommodate smaller sized control packets or it might use asynchronous operation. In this thesis, we only focus on slotted operation in the data plane. Although several node synchronization issues are noted for SOBS in regard with small scale fluctuations in the link propagation delays, resolutions to them are not studied in this thesis.

In SOBS, as soon as a burst is assembled at an edge ingress node, a BCP is sent in the control plane through the network to setup the optical path at each of the core nodes in advance. Then in the closest data slot after the required basic

offset time (for header processing at the intermediate nodes), the burst transmission is initiated. Although bursts are allowed in SOBS to vary in size depending on the assembly algorithm, we assume in this thesis that the burst length, L, is fixed and is an integer multiple of the slot length. We note the advantages of fixed burst sizes based on the findings of [14]. A SOBS implementation with $L > 1$ is a middle ground alternative between asynchronous OBS ($L \to \infty$) and SynOBS ($L = 1$) and yields some advantages which are discussed in Chapter 2.

Providing quality of service (QoS) to data bursts is one of the widely studied problems in OBS. In electronical packet switched networks, QoS is provided by means of per-class queueing, buffer management, and advanced scheduling mechanisms. However, lack of buffering limits the number of options for QoS provisioning in OBS networks. The most popular QoS technique for OBS is a prioritization technique in which high priority traffic is assigned longer offset times compared to low priority traffic [15]. For SOBS, the offset-based QoS technique reduces to sending high priority data bursts not right at the nearest data slot but at the next closest opportunity, which we call the unity-offset scheme. In case larger delays are tolerable for high priority traffic, one can optionally send the high priority data burst $T_{QoS} > 1$ data slots after the closest data slot. This scheme is called the nonunity offset scheme.

One other option for providing QoS in SOBS is that since the data bursts arrive at the same time, all BCPs arriving at the control plane corresponding to the bursts of the next data slot are processed together providing preferential treatment to high priority bursts. This mechanism is called priority scheduling in this thesis and we note that one does not need to use offset based differentiation in case $L = 1$ for a system with priority scheduling. When $L > 1$, priority scheduling and offset schemes can work in conjunction for improved preferential treatment for high priority traffic. We also limit the number of traffic classes to two in this study although some of the results are extensible to multiple

traffic classes. Motivated by Poisson arrival assumptions used commonly for asynchronous OBS systems, we assume that the number of reservation requests (for high and low priority traffic) arriving within a data slot and destined to a tagged fiber with W wavelengths is Poisson distributed. We also assume that arrivals within nonoverlapping slots are independent.

Vast majority of the research done on the synchronous OBS assumes bursts to last a single slot. To the best of our knowledge, the performance of SOBS with and without QoS mechanisms has not been extensively studied in the literature. Therefore, we develop a novel multi-dimensional Markov chain model of a multi-wavelength SOBS core node by which we quantify the variation of burst blocking probability with respect to the slot duration in a classless (best effort) network. Loss probability and slot duration are among the most important parameters in SOBS networks. Hence, both should be balanced carefully for a given set of service guarantees. Increasing/decreasing slot granularity/length shortens the delay that a packet experiences in the assembly queue since a ready burst no longer has to wait for a longer slot to be transmitted. On the other hand, decreasing the burst loss probability is of paramount importance in SOBS which suffers from high loss rates due to one-way reservation mechanism and lack of optical buffering.

Extending this Markov chain model, we also carry out performance analysis of a two-class SOBS core node. Three different prioritization schemes namely priority scheduling, unity-offset based differentiation and a combination of these two mechanisms are introduced and modeled. Then, a comparative analysis for these QoS schemes based on the corresponding burst blocking probabilities is given. In the analysis of unity-offset based differentiation scheme, Poisson distribution of the BCP arrivals is approximated with a phase type distribution using moment matching techniques proposed in [16], and the corresponding Markov chain is embedded into the mainstream Markov chain model of the core SOBS

node. Besides the numerical results of the thesis, this novel method is proposed as a useful tool for performance evaluation.

The rest of this thesis is organized as follows. In Chapter 2, after a brief introduction to optical switching paradigms, a detailed literature overview of OBS is given. In Chapter 3, the Markov chain model is constructed for a classless core SOBS node and the corresponding numerical results are presented. Then, in Chapter 4, this model is extended to analyze the three QoS schemes mentioned above in a two-class SOBS network and numerical results for these QoS mechanisms are presented. Finally in Chapter 5, we conclude the thesis and give a direction for future research.

Chapter 2

Literature Overview

Recent advances in wavelength division multiplexing (WDM) offer huge transmission capacity to optical networks (ONs) which carry the backbone traffic in the Internet. WDM is the technology by which data is transmitted through non-interfering data channels -wavelengths- over the same fiber link. The transmission capacity of a fiber link is simply given by the capacity of a single wavelength times the total number of wavelengths available for that link. Currently available industrial products have a channel transmission rate of up to 40 Gbps and more than 100 wavelengths per fiber.

This enhancement in the physical layer of the ONs has revealed the bottleneck in the network layer where optical data is traditionally switched/routed electronically via an opto-electro-opto (O-E-O) conversion. It is very difficult for electronic processing to keep up with the data speeds from multiple fiber links each operating in the order of Tbps. Moreover, an optical router having P ports and W wavelengths, needs a total of PW O-E-O converters which are expensive components. Transmitting data via these cross-domain transitions is called opaque way of transmission. In the long term, backbone traffic which is mostly transit is supposed to be carried in a transparent way without leaving the

optical domain. For that purpose, several switching paradigms proposed in the literature aim to transform the current opaque network architecture composed of point-to-point optical links into end-to-end transparent optical networks.

2.1 Optical Circuit Switching (OCS)

In OCS, transparency is achieved by pre-allocating dedicated wavelengths along each link from source to destination. This set of connected links is called a light-path, throughout which the data remains in the optical domain. A connection starts with a connection setup request message sent to the intermediate optical switches/routers. Each node tries to make the requested reservation and send back an ACK or NAK message according to the availability of its resources. Once a wavelength is reserved for a connection, it will not be available for any other attempts until a teardown message terminating the whole connection is received or a NAK message is received from the downstream nodes. As seen, OCS has a significant connection setup overhead since at least a round trip time passes before a successful circuit is established. This reservation protocol is called tell-and-wait as either a positive or negative feedback is expected before transmitting any data over the network. The ratio of the setup time to the total connection period directly gives the inefficiency of this approach. One way to reduce this overhead is to prolong the actual data transmission period making OCS impractical for applications requiring relatively small amount of data transfer. However, this would dramatically affect the statistical sharing of the links, and it is not compatible with today's constantly changing high-speed bursty traffic demands.

2.2 Optical Packet Switching (OPS)

OPS is the optical equivalent of the well-known electronic packet switching. Switching is done optically per packet which is the finest granularity in IP network layer. However, currently available optical technologies are immature to implement OPS [17], since no practical optical data processing and storage technology is available yet. Although some kind of optical buffering in terms of fiber delay lines (FDLs) exists, it lacks emulating RAMs and FIFO queues. Hence, unlike the electronic routers, buffering capacity can only be increased for a limited amount and functionality in order to alleviate blocking probabilities of packets. In a typical OPS network, O-E-O conversion is still required for packet header processing. Optical packets are demultiplexed from the fiber links and their headers are extracted to be processed separately. Meanwhile, the optical packet is delayed in FDLs until the switching fabric is configured properly according to the header information. An additional header insertion mechanism is needed to complete the forwarding action of the OPS switch/router. Note that, *PW* O-E-O converters are still needed, but possibly at a much lower speed.

2.3 Optical Burst Switching (OBS)

OBS [1] is a hybrid switching paradigm which offers data transparency and statistical sharing concurrently. In OBS, the smallest data unit is called a burst which is a collection of packets aggregated at the network edge. This enables switching to be done at the burst level decreasing the header processing overhead as compared to that of OPS. Also in OBS, O-E-O conversion is only required for a single dedicated control channel on each fiber link. On this separate channel, one-way reservation requests are sent prior to the burst transmission in order to allocate resources beforehand. This removes the necessity for indispensable FDLs of the OPS switches/routers. And after a predetermined amount of time,

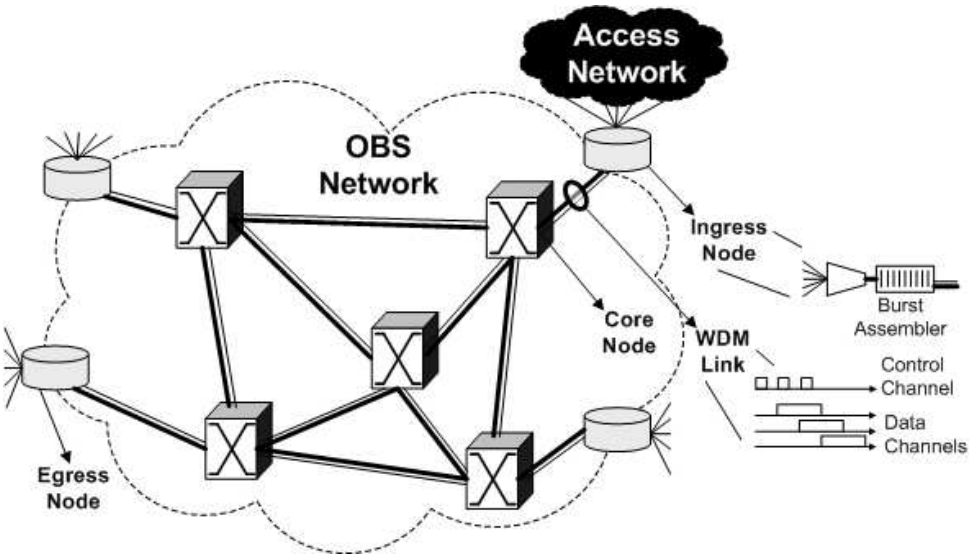

Figure 2.1: OBS network architecture

bursts are transmitted without waiting for a feedback from the network. By this way, no guarantee of burst delivery is given. However, for long-haul networks having large propagation delays higher throughput is obtained as compared to that of OCS [18]. This decoupling of the control and data planes in space and time, makes OBS an attractive switching paradigm by eliminating FDLs and exploiting the state-of-art electrical processing, optical transmission and switching capabilities. Next, the end-to-end transmission scenario of OBS is explained in detail.

2.3.1 OBS Network Architecture

In an OBS network shown in Fig 2.1, IP packets from different access networks destined to the same egress edge node are assembled into a burst at each ingress edge node. These burstified IP packets are recovered back by a process called de-assembly at the edge egress node. In the meanwhile, the burst remains in

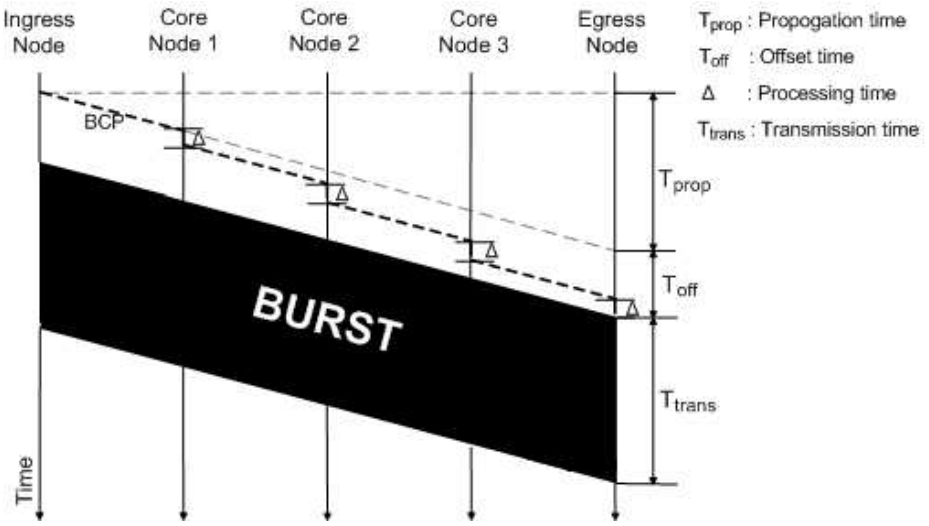

Figure 2.2: Timing diagram for a BCP and its burst in OBS

the optical domain as it traverses the OBS network. For that purpose, a burst control packet (BCP) is signalled out-of-band an offset time, T_{off}, before the prepared burst's transmission as seen in Fig 2.2. This BCP is processed and updated electronically by each intermediate core node and is used to adjust each switching matrix on the path so that the associated burst passes by in a cut-through manner. T_{off} is a function of the network topology and the average processing time per node, Δ, of BCP in the core nodes. For a given source-destination pair, the ingress edge node determines the number of intermediate nodes, H, including the final egress node by source routing. Then, it calculates the basic offset T_{off} as $H\Delta$. By doing so, BCP and the burst itself reaches the egress node simultaneously. Obviously, leaving an extra time margin between the BCP and the burst transmission relaxes this reservation mechanism against processing delay jitter. If the OBS network cannot accommodate the burst, it is simply dropped. Burst losses are not compensated with a backup mechanism at the ingress nodes, hence retransmissions are left to upper layer protocols.

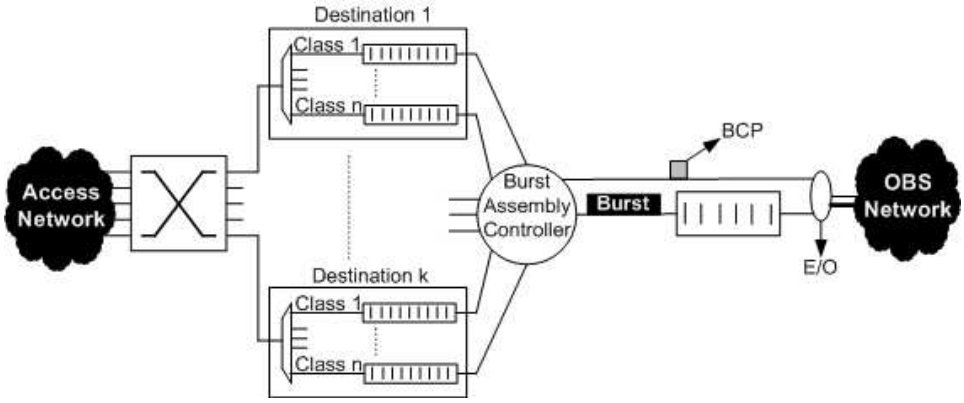

Figure 2.3: Ingress node architecture of OBS

2.3.2 Burst Assembly

At ingress nodes, IP packets are sorted based on their destination addresses and priority classes. For k destinations and n priority classes, kn queues are maintained as shown in Fig 2.3. Various burst assembly algorithms are deployed to create bursts out of these queues. Primary assembly algorithms are the timer based, burst-length based and the mixed timer/burst-length based ones.

In the timer based assembly scheme [19], a timer is reset at the beginning of each assembly cycle. When the timer reaches a timeout value, T_{to}, all packets arrived in this period are packed in a burst. The choice of T_{to} has a significant impact on the end-to-end network performance. A large value may not be tolerable for the TCP layer, the most widespread transport protocol in the Internet, whereas a small timeout may result in too small bursts increasing the switching and control overhead of OBS. While running a timer-based assembly algorithm, timers of different ingress nodes should be carefully de-synchronized in order to avoid subsequent burst collisions at the core nodes.

In burst-length based assembly scheme [20], a counter with an upper limit, l, in bytes, for the queued packets is used instead of a timer. When l is exceeded, enqueued packets are burstified and the counter is reset for the new coming packets. Burst interarrival times in OBS becomes highly sensitive to fluctuations in the packet arrival rates in this scheme. Especially under low traffic load, packets may experience long delays due to long burst assembly periods.

These assembly algorithms can also be used together in order to get rid of their drawbacks [21], [22]. In mixed timer/burst-length assembly algorithm, a burst is sent out when either a timer expires or a threshold for the aggregated burst length is reached.

Once a burst is generated, it is delayed by T_{off} in order to let its BCP reserve necessary resources in advance. OBS has not been standardized yet, so BCP format is not fixed. However it should at least convey the offset time, burst length, destination address and the priority class information to the core nodes for efficient resource allocation. Once fixed at the ingress node, burst length cannot be increased to make room for the arriving packets during this offset time as the downstream nodes cannot be informed about this update. However, there is a proposal to add the mean number of packets arriving to the node in the meantime, $l(T_{off})$ to l and to make the necessary reservations accordingly. If fewer packets than the estimated number arrive, bandwidth would be wasted. Otherwise, delay for those packets would be reduced by an assembly period.

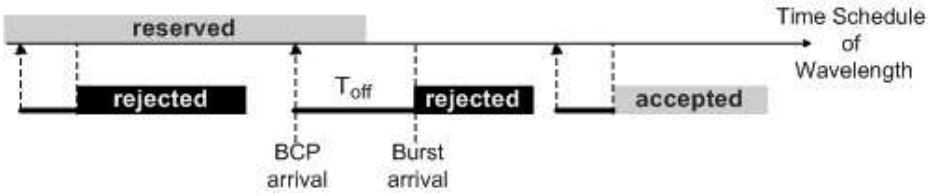

Figure 2.4: An example reservation scenario for IBT

2.3.3 Burst Scheduling

Scheduler is a hardware/software holding the availability status of the output wavelengths and managing reservations at the core nodes. It runs a burst scheduling algorithm to commit wavelengths to incoming bursts. Burst scheduling algorithms can be classified based on how the set-up and release information is used in the burst scheduler [23]. This classification is given as follows.

Inband Terminator

This approach offers a relatively low complexity algorithm to the scheduler. After an arriving BCP, the scheduler only checks the availability of wavelengths at the time being. Succeeding connections are then explicitly terminated by a trailing control packet indicating the end of burst transmission. Only the busy/idle states of the wavelengths are kept within the core node. Though very simple, this type of algorithms results in inefficient resource provisioning. A forthcoming burst whose BCP coincides with the busy period of a channel to be freed before the arrival instant of the burst itself is dropped which is depicted in Fig 2.4. Just-in-time (JIT) [24], [25], [26], [27] and tell-and-go (TAG) [28] scheduling mechanisms belong to this class.

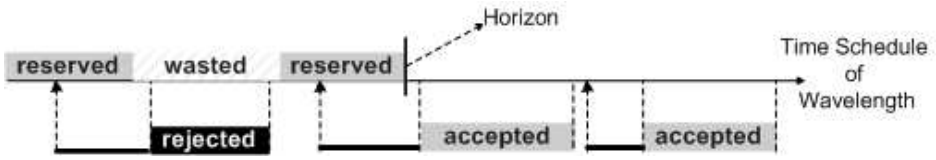

Figure 2.5: An example reservation scenario for RLD

Reserve Limited Duration

A more sophisticated but less wasteful burst scheduling approach incorporates knowledge of both offset and burst length while accepting or rejecting bursts. Horizon [29] and Latest Available Unscheduled Channel (LAUC) [30] algorithms keep a horizon for each wavelength. Horizon is the instant after which the wavelength will be idle. Fig 2.5 depicts that a wavelength can be assigned to a burst if its horizon is earlier than the burst's arrival time. If so, the horizon is updated to the departure time of that burst which is its burst length plus offset length. As a drawback, Horizon and LAUC inevitably leaves wasted gaps between bursts especially when burst offsets and lengths become comparable in length.

Reserve Fixed Duration

Reserve fixed duration (RFD) algorithms are the most advanced ones which keep record of all start and end times of burst transmissions or alternatively the gaps in between. Instead of immediately reserving a channel to an eligible incoming burst, a delayed reservation protocol is run by which other bursts that possibly fit in gaps are also evaluated for the same channel as shown in Fig 2.6. Unlike the Reserve Limited Duration scheme, RFD permits reservations not only after the horizon but also before it. LAUC with void filling (LAUC-VF) [22] and just-enough-time (JET) [1] are the proposals for that kind of mechanism. Also

Figure 2.6: An example reservation scenario for RFD

variants of LAUC-VF [31], minimizing the starting (Min-SV), the ending (Min-EV) and the total of starting and ending (Best Fit) gaps exist.

All these burst scheduling algorithms converge to each other as the offset length in the optical network goes to zero. In [23], [32] and [33], these reservation mechanisms are comparatively evaluated.

2.3.4 Contention Resolution

OBS suffers from contention due to its one-way reservation mechanism and bufferless nature. Bursts may experience high loss rates due to conflicting requests for the same outgoing wavelengths at the core nodes. Contention can be resolved by uniformizing this traffic demand in either space, wavelength or time domain. These methods remedy the shortage of resources at the expense of some associated hardware cost.

In wavelength conversion, carrier wavelengths of the contending bursts are changed through wavelength converters (WCs) in the optical switches before directed to the output ports. The capability of full wavelength conversion (FWC) is used for switches ensuring a one-to-one conversion among all wavelengths where partial wavelength conversion (PWC) [34] is used for switches lacking this flexibility due to scarcity of WCs. Although FWC is advantageous for efficient sharing of bandwidth, it increases cost and complexity of the switches. On the other

hand, PWC cannot save a contending burst even if an idle wavelength exists when all WCs are busy.

As a time domain resolution, bursts can be time shifted by means of FDLs until the contention is resolved. In [35], it is claimed that FDLs should be a few multiples of mean burst length for satisfactory loss rates. Burst durations can range from tens of microseconds to milliseconds as far as the current switching and processing technology is concerned, leading to fiber cable rolls of a few to hundreds of kilometers. However, FDLs have some physical limitations in maximum length due to chromatic dispersion and power dissipation unless fiber amplifiers are incorporated. FDLs can be categorized into single-stage and multi-stage structures in which delay granularity is reached by parallel fixed sized FDLs or cascaded FDLs respectively. They are also differentiated with respect to their positioning in the switches as feed-forward (FF) and feedback (FB) [36]. Bursts are looped back to a previous stage of the switch in FB FDLs where they are passed through a next stage in FF FDLs.

Wavelength conversion and buffering can be used together to effectively workaround contention [34], [35]. In this way, less WCs and lower degree FDLs may become sufficient. In Fig 2.7, a core node equipped with both FB FDLs and FWC is pictured.

In deflection routing [37], [38], [39] a space domain resolution to contention, contending bursts are forwarded to predetermined alternative ports. These bursts follow secondary paths to their destinations. However, for high traffic load, deflected bursts start to contend with the other bursts on their primary paths shifting them to secondary paths as well. This trend results in sub-optimal link utilization degrading the OBS performance. Other problems such as offset time compensation for the new route [40], infinite loops in the network, increased latency and out-of-order packet delivery regarding the TCP layer, should also be taken into account while implementing deflection routing.

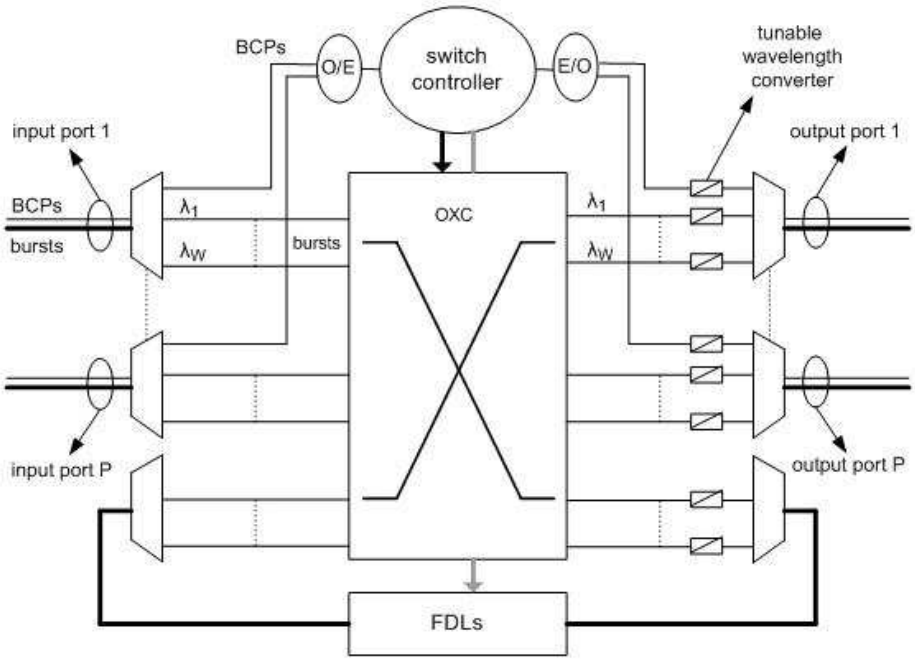

Figure 2.7: A typical OBS core node

If none of these methods succeed in resolving contention, then the contending bursts are either fully or partially dropped. Partial dropping is called burst segmentation [41], [42], [43], where segments of either head of the contending or the tail of the original burst are dropped. Segments are subdivisions inside a burst consisting of several or more IP packets. Burst segmentation increases the control overhead in bursts besides introducing small bursts into the OBS network.

2.3.5 Quality of Service (QoS) in OBS

In the field of computer networking, QoS is the ability to generate different priority classes among data flows by guaranteeing a certain level of performance. In its early stages, Internet was delivering best effort traffic to users due to poor processing power of routers. In time, emerging real-time streaming multimedia

applications such as Voice over IP (VoIP), Video Teleconferencing (VTC) and demand for prioritized links over the public connections have valued the QoS concept. These applications requiring lower layer internet protocols to ensure a minimum bit rate and a maximum delay are denominated as inelastic. On the other hand, HTTP and FTP applications are mostly elastic as they can still keep operating even under inferior network conditions. Possible metrics for QoS are end-to-end network delay, delay jitter, bit error rate, frequency of out of packet delivery and packet loss rate.

In OBS, end-to-end delay of a packet between the ingress and the egress nodes is T_{ass} (burst assembly delay) + T_{off} (offset delay of the burst) + T_{trans} (transmission delay of the burst) + T_{prop} (end-to-end propagation delay of the network) + T_{de-ass} (burst de-assembly delay) assuming no FDLs are used inside the core network. T_{trans}, which is negligible in optical communications, and T_{prop} are common to traditional networks as well. Remaining T_{ass}, T_{off} and T_{de-ass} are design parameters of OBS which can be fine-tuned for a specific QoS class. Moreover, bursts do not experience highly varying delays in OBS. In the absence of queuing at the core nodes, delay jitter is mainly affected by the burst assembly period T_{ass} which can also be kept constant by running timer-based burst assembly algorithms. Probability of bit error in optical transmission is far too low as compared to electronic transmission. Also, out-of-order packet delivery which deteriorates the end users' TCP performance can be avoided if deflection routing and FDL usage are omitted for contention resolution. Then remains the major problem of OBS, high burst loss rates caused by contention. Increasing buffer capacity in electronic networks is the ultimate solution to avoid packet loss. However, it is not applicable to OBS. Thus some other methods have been proposed in the literature to resolve contention. These contention resolution schemes can be modified to favor one class of burst against another so that multiple QoS classes are supported by an OBS network. Next some of them are qualitatively discussed with their pros and cons.

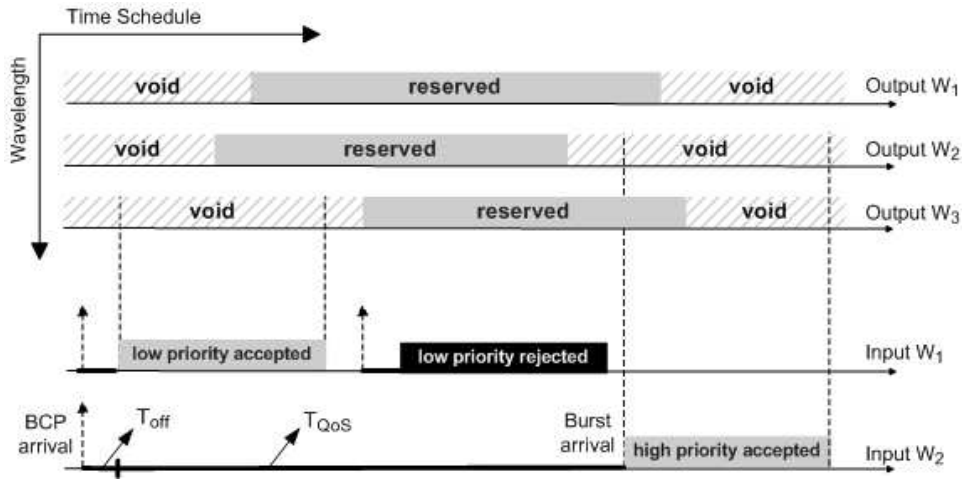

Figure 2.8: An example scenario for offset-based QoS

Offset Based Differentiation

Intuitively, privilege to make reservation for a further moment in time than the other competing agents, increases the chance of finding an available resource for that moment. Similarly, in offset based differentiation [44], [45], a high priority ready-to-transmit burst is delayed by an extra QoS offset, T_{QoS}, in addition to its basic offset T_{off}. It is shown in [44] that, when T_{QoS} is in the order of a few mean low priority burst length, l_{lp}, considerable degree of isolation between high and low priority class bursts can be achieved. Especially, when T_{QoS} exceeds the maximum burst length plus the maximum offset length of low priority bursts, high priority bursts no more see any low priority bursts and perfect isolation between classes is achieved at the expanse of increased end-to-end delay. However, this strategy does not scale in the number of supported QoS classes, as extra offsets grow exponentially w.t.o prioritization degree. These large QoS offsets which are very sensitive to l_{lp}, may not be balanced out by the attained low blocking rates for high priority classes [46].

From the low priority perspective, they try to fit in the gaps created by high priority bursts as shown in Fig 2.8. Hence usage of RFD based scheduling algorithms such as LAUC-VF or JET becomes a must. This QoS scheme also leads to a length selective characteristic of OBS favoring smaller low priority bursts having more chance to fit in small gaps left by the high priority bursts.

Intentional Burst Dropping

A distributed admission control mechanism called intentional burst dropping is introduced in [47] as an alternative to offset based differentiation. It actively controls the proportional burst drop rates at each core node and proportional assembly delay at each ingress node. Since no extra QoS offset is used, total network delay mainly consists of the assembly time. In this work, q_i and s_i are chosen for the QoS metric and the differentiation factor of the i-th priority class respectively. Then an algorithm is proposed to satisfy the following relation:

$$\frac{q_i}{q_j} = \frac{s_i}{s_j}. \tag{2.1}$$

In the algorithm, arrival and loss statistics of each QoS class are recorded at the core nodes and as long as a class is under its proportional loss rate, the bursts in that class are intentionally dropped. A core node performing this functionality is shown in Fig 2.9. Similarly delay statistics of IP packets at the ingress nodes are used to provide with a proportional QoS for delay.

This technique proactively discards lower priority bursts before contention. When no higher priority burst arrives to the node, then that lower priority bursts would have been needlessly discarded reducing the wavelength utilization. Also, since no absolute QoS is delivered to the bursts, loss rates of individual priority classes have great impact on the overall loss rates.

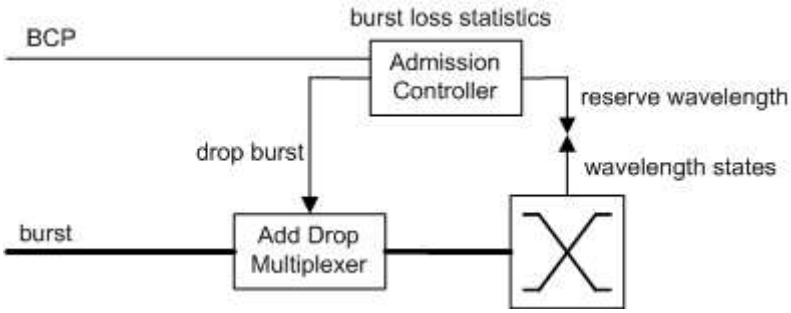

Figure 2.9: Functional block diagram of a core node for intentional burst dropping based QoS

Burst Segmentation and Deflection

[42] develops a QoS policy incorporating both tail-segmentation and deflection as follows. Contending high priority bursts always segment the in-service low priority bursts regardless of their length. The segmented part of the low priority bursts are then deflected through an alternative port if available, otherwise, they are dropped. Low priority bursts are entirely deflected or dropped when they contend high priority bursts. Intra-class contentions between the contending burst and the remaining part of the original burst are resolved by prioritizing the longer one according to the aforementioned rules. While dropping the tail of a burst, reconfiguration time of the switching matrix should also be considered as shown in Fig. 2.10. It is clear from the figure that, lower switching time results in less segment losses from the in-service burst increasing the efficiency of this contention resolution scheme.

Like in intentional dropping, high priority bursts do not experience a significant network delay in burst segmentation and deflection. Full isolation between QoS classes can be achieved. However, as the network load increases the carried traffic tends to be comprised of small fragmented bursts which in turn increases

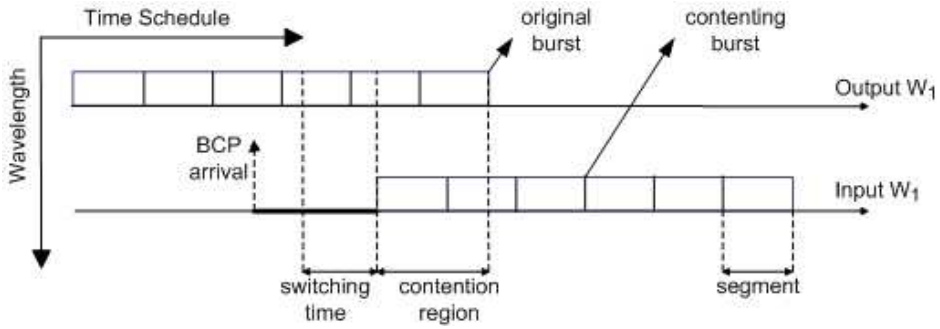

Figure 2.10: An example scenario for burst segmentation based QoS

the switching overhead. Also significant complexity is imposed on the core nodes as they have to make on-the-fly segmentation, prepare new BCPs for the new segments, and send trailer packets for the original bursts in order to inform downstream nodes about the segmentation.

Priority Scheduling

Priority scheduling, also referred as priority queue based differentiation in [48], is managing burst transmission requests according to their priority levels rather than a first-come-first-serve basis. In [49], a generalized LAUC-VF (G-LAUC-VF) algorithm is proposed in which BCPs of different QoS classes are separately queued at each core node. After regular time periods called slots, the schedulers at the optical nodes serve these BCP queues by executing the legacy LAUC-VF algorithm beginning from the highest priority to the lowest one. Hereby, each QoS class is given a strict priority over the lower ones within a slot. By building G-LAUC-VF on top of LAUC-VF, the algorithm is kept at a feasible complexity, but additional processing delays are introduced especially to lower priority burts.

2.3.6 Synchronous OBS

A comprehensive overview of OBS is given for its asynchronous mode of operation in the previous sections. Like every communication system, OBS can receive and transmit data synchronously in data slots. Data slots are separated by a guard time period to allow for switching matrix state transitions and to handle synchronization errors caused by chromatic dispersion, desynchronized local clocks, etc. Time-sliced OBS (TSOBS), Slotted OBS (SOBS), Time-synchronized OBS (SynOBS) have been the main three variants of synchronous OBS introduced in the literature so far and are briefly introduced next.

TSOBS

In TSOBS [50], burst transmissions are time-division-multiplexed (TDM) in order to break the dependency on costly WCs (wavelength converters) [51] for statistical sharing of available bandwidth. Hereby, TSOBS replaces switching in wavelength domain with switching in time domain. Data wavelengths carry bursts over repeating frames which are subdivided into fixed size time slots. A time slot at a fixed position within consecutive frames is called a channel. Burst switching in TSOBS corresponds to assigning an outgoing time slot to an incoming burst. This requires the ability to change the burst's channel making the optical buffering in TSOBS switches/routers mandatory. Optical time slot interchangers (OTSIs) are the blocks used to perform this functionality. The amount of FDLs inside, the size of the internal crossbar and the average number of switchings per burst are key design criteria for OTSIs.

TSOBS has a very similar transmission protocol compared to traditional OBS. It retains the one-way reservation scheme with dedicated control plane carrying the BCPs (so-called burst header cell, BHC in [50]). BCPs are transmitted an offset time ahead of the bursts and they contain the destination address,

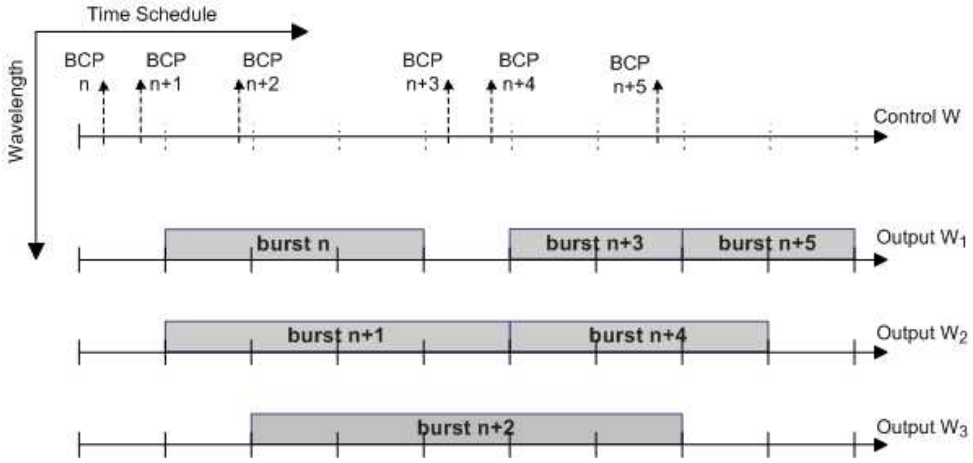

Figure 2.11: BCP and burst transmissions in SOBS

wavelength, channel, offset and the length of the incoming burst. Offset and length are measured in terms of frames. Since TSOBS is out of the scope of this thesis, it will not be discussed further.

SOBS

In SOBS [11], data and control plane are divided into time slots, where bursts can be of either a single or a multiple number of slots in duration. Control plane is further divided into smaller slots in order to accommodate smaller sized control packets. Despite of this definition, control plane can be operated asynchronously since synchronizing very small slots may have diminishing return due to stringent timing requirements and guard time inefficiency. Fig. 2.11 demonstrates a typical transmission scenario in SOBS. Unlike TSOBS, wavelength conversion is used for resource multiplexing instead of TDM. SOBS is the discrete counterpart of asynchronous OBS. This relation is analogous to the one between the well-known slotted ALOHA and ALOHA.

As soon as a burst is assembled at an ingress node of the SOBS network, a BCP is sent in a control plane slot through the network to setup the optical path at each core node in advance. Then in the closest data slot after the required basic offset time for header processing at the intermediate nodes, burst transmission is started. Depending on the assembly algorithm, bursts are allowed to vary in size. A BCP of SOBS network carries information about the destination address, length, offset time and the carrier wavelength of the burst to the core nodes. Scheduling algorithms as well as contention resolution schemes of traditional asynchronous OBS networks are still applicable to SOBS networks.

SynOBS

SynOBS [52] is another synchronous mode of OBS in which bursts have single slot duration and wavelength conversion is enabled to increase the multiplexing capacity of the optical network. SynOBS is a convergence of SOBS and TSOBS as far as these two changes are respectively considered. The choice of the slot duration in SynOBS is an optimization problem and analyzed in [53]. Decreasing the slot length decreases the link efficiency as guard period becomes comparable with the slot period. On the other hand, increasing the slot length increases the chance of partially filled slots generated by the burst assembly algorithm.

Comparison of Synchronous and Asynchronous OBS

Both synchronous and asynchronous OBS have advantages and disadvantages on their own right. These are listed as follows.

1. Asynchronous OBS, being relatively easy to implement, has high blocking probability due to its unpredictable burst arrival characteristics. For example, one of the two bursts destined to the same channel may be entirely dropped even if they are partially overlapped. This certainly reduces the

link efficiency in OBS networks. To the contrary, in SynOBS, contending bursts either completely or never overlap with each other. SOBS lies in between SynOBS and asynchronous OBS in terms of blocking performance, since bursts may be spread over multiple slots.

2. Synchronous OBS networks have a well-known synchronization problem of incoming bursts, as out-of-phase arrivals to the switching matrix are not acceptable. Temperature variations and chromatic dispersion [54] along fiber links are two main reasons for such phase differences between the carrier wavelengths. As a typical example for chromatic dispersion, a delay variation of 20ps/nm/km results in 2.4 microseconds delay between two wavelengths having 120 nm spectral distance over a 1000 km fiber cable. Propagation delay of light further differs in 1.2 microseconds for a temperature gradient of 30 °C over the same fiber with a 40/ps/°C/km delay variation. However, delay compensators can be used to remove these physical impairments since they are quite static w.r.t. time. Clock synchronization among the network is another issue that should also be well taken care of. As a final remedy, guard periods are left between the data slots improving the stability of the synchronous OBS networks at the expense of reduced link utilization.

3. IP packets gathered from synchronous and asynchronous access networks are subject to a delay of T_{ass}, assembly delay, at the edge of the OBS networks. In addition to T_{ass}, in synchronous OBS, they experience another delay before their encapsulating bursts are injected into the network. As bursts are transmitted only at the slot boundaries, a burst whose aggregation finishes just after a slot edge is transmitted after a full slot period. For a fixed burst length, slots of SynOBS are multiples of that of SOBS having a multiplicative effect on this additional latency of bursts at the network edges. Diminishing slot length in SynOBS, can reduce this latency at the expense of reduced link utilization due to guard periods between

slots [53]. On the other hand, in traditional asynchronous OBS networks ready bursts can immediately be sent into the network a basic offset time after their BCPs.

4. Synchronous arrivals of bursts mitigate the effect of internal blocking of optical switches [13], [55]. More specifically a rearrangably non-blocking switch can be made to function as a strictly non-blocking one in a Syn-OBS network. Once configured on the slot boundary, no further update is needed until the next slot, which is not the case in asynchronous OBS. Hence less stringent connectivity requirements can be imposed on switches which in turn may decrease the inefficiency originating from the synchronization. SOBS has a relatively small loss performance improvement over asynchronous OBS as compared to SynOBS.

5. A major cost of synchronous operation in OBS is the necessity of additional fiber delay lines (FDL) appended to each link [13]. However if the slot length is chosen to be small, the required FDL length will be small as well. On the other hand, decreasing the size of a slot has a drawback if the bursts are transmitted only in a single slot (SynOBS), since the guard periods for switching will cause inefficiency in the link utilization. At this point, taking burst lengths a few multiples of the slot lengths hence adjusting the granularity of these slots independent of the burst length may be desirable.

6. In synchronous OBS, the scheduler always has the freedom of serving the higher priority bursts first. As it receives the BCPs for a specific slot, the scheduler of the core node can reconfigure the switching matrix so that available resources are all offered to high priority bursts. This scheme is denoted as priority scheduling throughout this paper [13]. Priority scheduling is not well-suited to asynchronous OBS because of its unpredictable burst arrival times. On the other hand, it certainly does not fully isolate the QoS classes in SOBS, since lower priority bursts in service still can block

higher priority ones if the burst lengths are of multiple data slots and no segmentation based technique is deployed. Unlike SOBS, SynOBS takes full advantage of priority scheduling in isolating the QoS classes.

7. In synchronous OBS, the timing information is always in the units of slots. [13]. However, in asynchronous OBS, control packets have to carry the exact time of burst arrival and burst length which requires space in bytes. Shorter control packets in synchronous OBS, reduces the level of control plane congestion.

8. A SOBS node needs to make scheduling decisions for all bursts coming in a given slot. Since the time required to run a scheduling algorithm is rather limited, it might be appropriate to reduce the number of bursts for which a scheduling decision is to be made. A reduction factor of burst length is possible for SOBS relative to SynOBS as long as the traffic load of the network is kept constant. In asynchronous OBS, scheduling is done continuously relaxing the timing requirements of the scheduling algorithms.

In this thesis, we concentrate on the SOBS paradigm where burst length to slot length ratio is nonunity. In the next Chapter, we present a Markov chain based framework for the analysis of a classless SOBS node and seek performance gains of SOBS over asynchronous OBS. In the other chapter, we extend this framework to the analysis of QoS with priority scheduling and unity-offset; analyze the scenario when both priority scheduling and unity offset-based QoS differentiation is employed; and use regression to approximate the case of nonunity offsets.

Chapter 3

Burst Blocking Probability Analysis of a Classless SOBS Node

In this chapter, the SOBS node whose data stream is depicted in Fig. 2.11 is modeled. For this node, we assume all BCPs arrive according to a Poisson process with rate λ where each BCP corresponds to a burst with a constant length of L data slots. This assumption implies that the burst offsets due to processing delays at intermediate core nodes should be much smaller than a single data slot. As the optical node resembles a first-in-first-out server with this assumption, all three scheduling algorithms introduced in Section 2.3.3 prove to be equivalently efficient. However, RLD based Horizon algorithm is chosen as the framework of this study as it is simple but suitable for handling non-negligible offsets between the BCP-burst couples. We further assume FWC (full wavelength conversion) capability among the W wavelengths of the core node, meaning that bursts on any incoming wavelength are eligible to be switched through any outgoing idle wavelength. As will be clear in this section, FWC removes the necessity for individually tracking wavelengths and allows to group the ones having the

same horizon while constructing the Markov chain. Other contention resolution methods such as deflection routing, segmentation and FDL usage are beyond the scope of this thesis.

3.1 Markov Chain Model

For the described optical node, there are at most L different groups of horizon each of which is denoted as s^i, where s^i is the number of channels that will be occupied for i slot(s) from the current slot and $i \in \{0, 1, \ldots, L-2, L-1\}$. s^0 is the number of idle channels in the current slot. Since an immediately scheduled burst will have $L-1$ slots left to be transmitted on the next slot epoch, upper limit for i is $L-1$. A state $\bar{\mathbf{s}}$ of the L-dimensional Markov chain Q can be written as $\bar{\mathbf{s}} = (s^0, s^1, \ldots, s^{L-2}, s^{L-1})$, where $\bar{\mathbf{s}}$ is the descriptor of the optical node in terms of the availability status of its wavelengths w.r.t. time. The total number of states of Q, N, is given by the number of distinct solutions to

$$\sum_{i=0}^{L-1} s^i = W, \tag{3.1}$$

where $s^i \geq 0$. N can be calculated from (3.1) as

$$N = \binom{W+L-1}{W}. \tag{3.2}$$

Each solution of (3.1) is a state $\bar{\mathbf{s}}$ of the Markov chain Q. Note that, if FWC assumption were not used, Markov chain model of the system would have a reachable state space size of L^W. However, FWC capability of the SOBS node allows grouping of wavelengths and thus reduces this state space size to N. For $W = 10$ and $L = 5$, L^W and N are equal to 9765625 and 1001 respectively.

Once states are enumerated according to (3.1), the transition matrix $T_{N\times N}$ of Q can be calculated from Table 3.1 where all possible transitions from a state $\bar{\mathbf{s}}$ conditioned on its substate s^0 are shown. Transition conditions in this table

Current State $\bar{\mathbf{s}}[n] = (s^0, s^1, \ldots, s^{L-2}, s^{L-1})$		
Next State $\bar{\mathbf{s}}[n+1] =$	**Transition Condition**	**Transition Probability**
$(s^0 + s^1 - i, s^2, \ldots, s^{L-1}, i)$	$i < s^0$	$q_{(i)}$
$(s^1, s^2, \ldots, s^{L-1}, s^0)$	$\forall i \geq s^0$	$\sum_{k=s^0}^{\infty} q_{(k)} = X_{(s^0-1)}$

Table 3.1: State transitions from a given state $\bar{\mathbf{s}}$ of the Markov chain Q of a classless SOBS node

indicates that as long as incoming number of bursts, i, is less than the available number of channels, s^0, s^{L-1} becomes i. Otherwise, excessive bursts are dropped keeping s^{L-1} at a maximum of s^0. Another action in state transitions is the left-shifting of all states. Since each transition occurs between subsequent data slots, this shift operation corresponds to advancing in time. The number of burst arrivals in a slot is Poisson distributed with rate λ and the transition probabilities in Table 3.1 are expressed in terms of its PMF, CDF and complementary CDF (CCDF) functions which are respectively defined as:

$$q_{(i)} := \frac{e^{-\lambda}\lambda^i}{i!}, \tag{3.3}$$

$$F_{(k)} := \sum_{i=0}^{k} q_{(i)}, \tag{3.4}$$

$$X_{(k)} := \sum_{i=k+1}^{\infty} q_{(i)}. \tag{3.5}$$

Q is irreducible, since every state $\bar{\mathbf{s}} = (s^0, s^1, \ldots, s^{L-2}, s^{L-1})$ communicates with every other state $\bar{\mathbf{s}}' = (s^{0'}, s^{1'}, \ldots, s^{L-2'}, s^{L-1'})$ in Q, whose proof is as follows. With probability ${q_{(0)}}^{L-1}$, no burst arrives to the system in $L-1$ consequent data slots, which corresponds to an $L-1$ step transition to the state $\bar{\mathbf{s}} = (W, 0, \ldots, 0, 0)$. Then, with probability $q_{(s^{1'})}q_{(s^{2'})}\ldots q_{(s^{L-2'})}q_{(s^{L-1'})}$, $s^{1'}$ up to $s^{L-1'}$ number of bursts arrive to the system in the next $L-1$ consequent data slots corresponding to an $L-1$ step state transition to the sate $\bar{\mathbf{s}}' = (s^{0'}, s^{1'}, \ldots, s^{L-2'}, s^{L-1'})$. In Q, the state $\bar{\mathbf{s}} = (W, 0, \ldots, 0, 0)$ has a transition to itself with probability $q_{(0)}$, which means this state is aperiodic. For an

irreducible Markov chain, it is a sufficient condition to have one aperiodic state to be aperiodic. Therefore, Q is also an aperiodic Markov chain.

Let π be the equilibrium distribution of this aperiodic and irreducible Markov chain Q, and $\pi(\bar{\mathbf{s}})$, where $\bar{\mathbf{s}} \in Q$, be the steady state probability of state $\bar{\mathbf{s}}$. Then the following equations must be satisfied:

$$\pi T = \pi, \tag{3.6}$$

$$\sum_{\bar{\mathbf{s}} \in Q} \pi(\bar{\mathbf{s}}) = 1. \tag{3.7}$$

Burst blocking (loss) probability of this optical node is then given by

$$P_{loss} = \frac{\text{E\{ \# of burst drops in a slot \}}}{\text{E\{ \# of burst arrivals in a slot \}}} = \frac{\sum_{\bar{\mathbf{s}} \in Q} \pi(\bar{\mathbf{s}}) \mu(\bar{\mathbf{s}})}{\lambda}, \tag{3.8}$$

where $\mu(\bar{\mathbf{s}})$ is the expected number of burst drops in a definite state $\bar{\mathbf{s}} = (s^0, s^1, \ldots, s^{L-2}, s^{L-1})$ which is given by

$$\begin{aligned} \mu(\bar{\mathbf{s}}) &= \sum_{i=s^0+1}^{\infty} q_{(i)}(i - s^0) \\ &= \sum_{i=s^0+1}^{\infty} \frac{e^{-\lambda}\lambda^i}{i!} i - s^0 \sum_{i=s^0+1}^{\infty} q_i \\ &= \sum_{m=s^0}^{\infty} \frac{e^{-\lambda}\lambda^{m+1}}{m!} - s^0 \sum_{i=s^0+1}^{\infty} q_i \\ &= \lambda X_{(s^0-1)} - s^0 X_{(s^0)}. \end{aligned} \tag{3.9}$$

Figure 3.1 is an example Markov chain model of a classless core SOBS node with $W = 3$ and $L = 2$. Figure 3.2 shows how state transitions occur in this Markov chain for a series of burst arrivals. In Figure 3.2, wavelength occupancy is shown both before and after the slot boundaries. However, the presented Markov chain only keeps track of the former one saving from one redundant state. As seen in the figure, none of the server's horizon extends beyond one slot when observed before the slot boundaries, while it is not true otherwise.

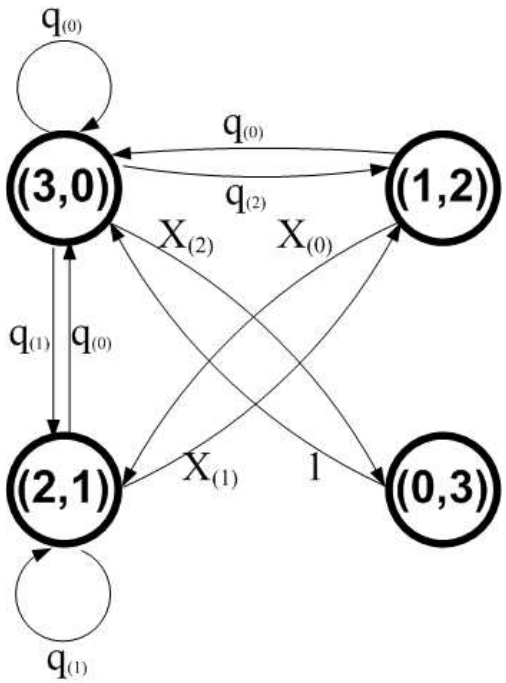

Figure 3.1: An example Markov chain with $W = 3$ and $L = 2$

Since parameter L is the ratio of the burst length to the slot length, variations in L can also be interpreted as variations in the slot duration. In this part of our analysis, we seek the effect of slot granularity over the burst blocking probability. In other words, we assess the penalty of spreading bursts over several slots while keeping their absolute length constant. In the limiting case where slot length becomes infinitesimal, the SOBS node under consideration behaves as an $M/M/C/C$ loss system with $C = W$ servers and offered load $\rho = \lambda/W$; λ corresponds to the burst arrival rate when burst duration equals slot duration (i.e., $L = 1$).

In the pure slotted case (SynOBS), where $L = 1$, the Markov chain Q has a single state according to (3.1) in which all wavelengths are available. In this network configuration, burst transmissions last only one slot and the whole system returns to its idle state on every slot epoch. The burst blocking probability for

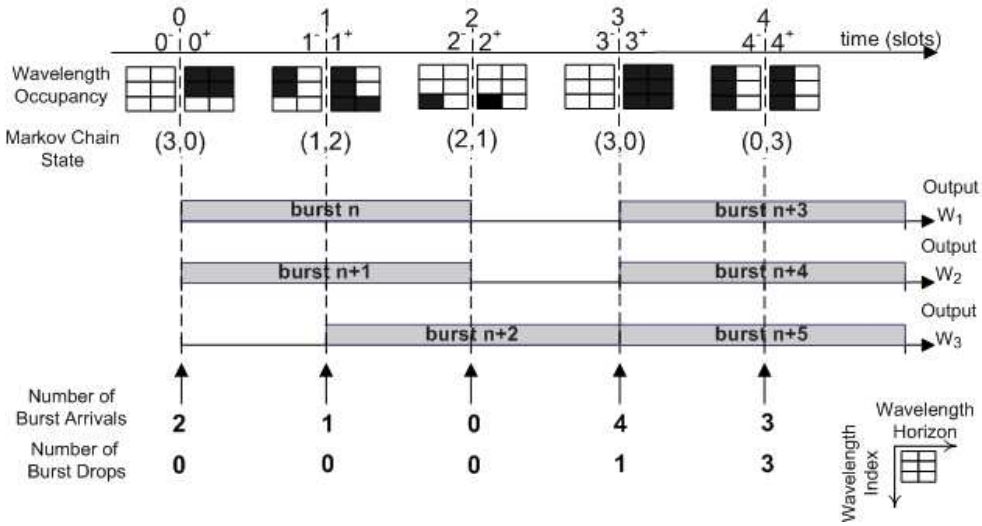

Figure 3.2: Timing diagram of the SOBS node in Fig. 3.1

this case is given by the simplified version of (3.8) as follows:

$$P_{loss} = \frac{\mu(\bar{\mathbf{s}})}{\lambda} = \frac{\lambda X_{(W-1)} - W X_{(W)}}{\lambda}. \tag{3.10}$$

(3.10) is also derived by [12] for the performance analysis of a core SynOBS node without FDLs. When L is larger than 1, in order to keep ρ constant the following equation is used to derive λ of the corresponding system:

$$\lambda = \frac{\rho W}{L}. \tag{3.11}$$

.

3.2 Numerical Results

In this chapter, we have presented a Markov chain model for a core SOBS node with burst transmissions lasting either a single-slot (pure-slotted) or multi-slots. In Figure 3.3, the proposed analytical model is tested against simulations for

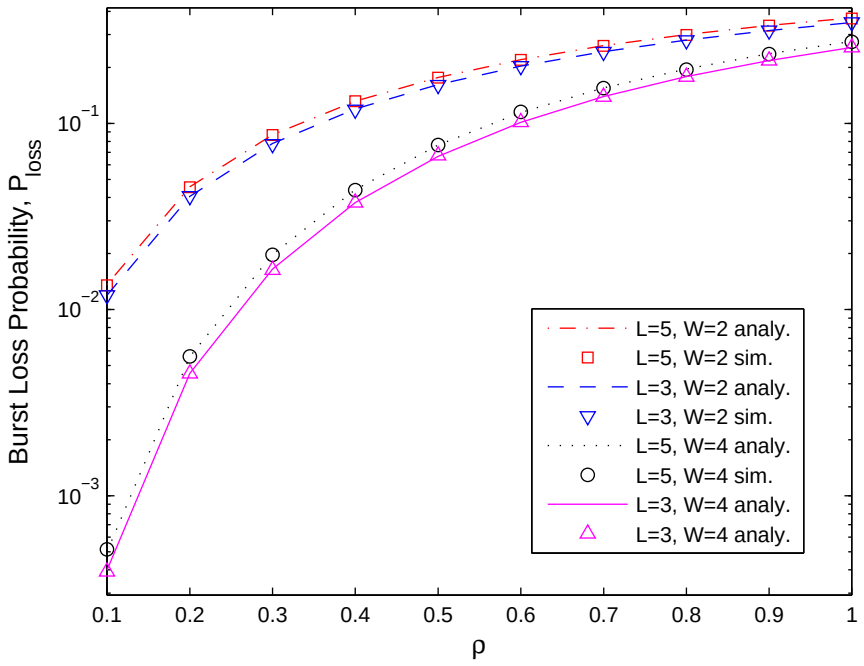

Figure 3.3: Analytical and simulation results for burst loss probabilities of a classless SOBS node

various L, W and ρ. All numerical evaluations and corresponding simulations of the analytical models throughout this thesis are done in C/C++ programming language and for linear algebra computations an open source package [56] is used.

We graphically compare the burst blocking probabilities of the $M/M/C/C$ (slot length=0), the pure-slotted (slot length=L) and the multi-slotted servers with different slot durations in Figures 3.4(a) and 3.4(b) for $W = 2$ and $W = 8$, respectively. As expected, irrespective of traffic load and number of wavelengths, there is a convergence of the multi-slotted server to the $M/M/C/C$ server as the slot length becomes smaller and smaller. Definitely as the arrival characteristics of bursts become more unpredictable, burst blocking probability of the node increases which is the observed trend in the figures. To the contrary, as the slot length reaches the burst length, server attains its lowest burst blocking probability. Both Figures 3.4(a) and 3.4(b), yield a gap between the two distinct mode of operations less than an order of magnitude. It is seen form the results that

the performance of the multi-slotted server lies in between the pure-slotted and the $M/M/C/C$ servers.

In Figures 3.5(a) and 3.5(b), blocking probabilities are plotted as a function of the effective burst length, L, which is the burst length divided by the slot length. Dashed lines above each curve are drawn for the corresponding $M/M/C/C$ server performance. These figures reveal that the proportional gap between pure-slotted server and $M/M/C/C$ server increases as the wavelength W increases and load ρ decreases. Consequently, performance gain of synchronizing the OBS network is more prominent for lower loss rates. In Figure 3.5(a), note that an SOBS configuration of $W = 6$ and $L = 2$ yields the same performance with that of the asynchronous OBS having $W = 8$. A similar observation can be made in Figure 3.5(b), as an SOBS node provides with a lower loss rate as compared to an asynchronous OBS. In other words, an SOBS node can carry higher volumes of traffic than an asynchronous OBS with the same P_{loss}.

Presenting the analysis results for the multi-slotted system, possible QoS methods for SOBS are analyzed using the Markov chain models in the next chapter.

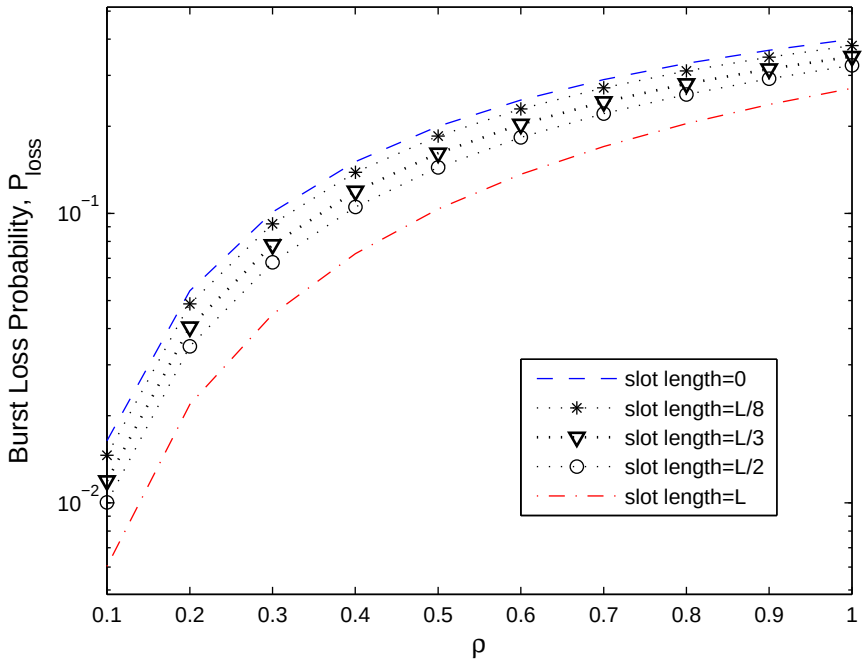

(a) W=2

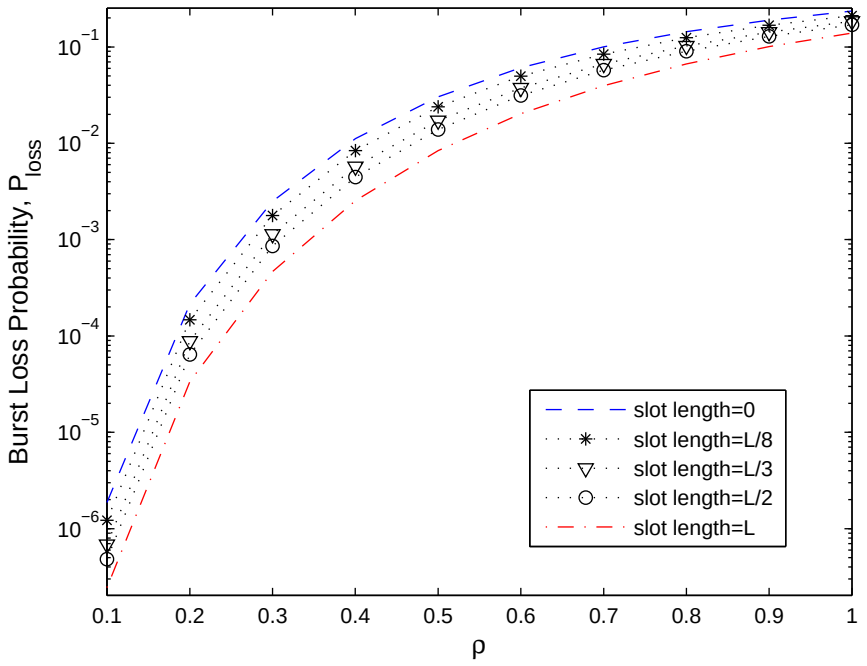

(b) W=8

Figure 3.4: Burst loss probabilities of a classless SOBS node for different values of slot length

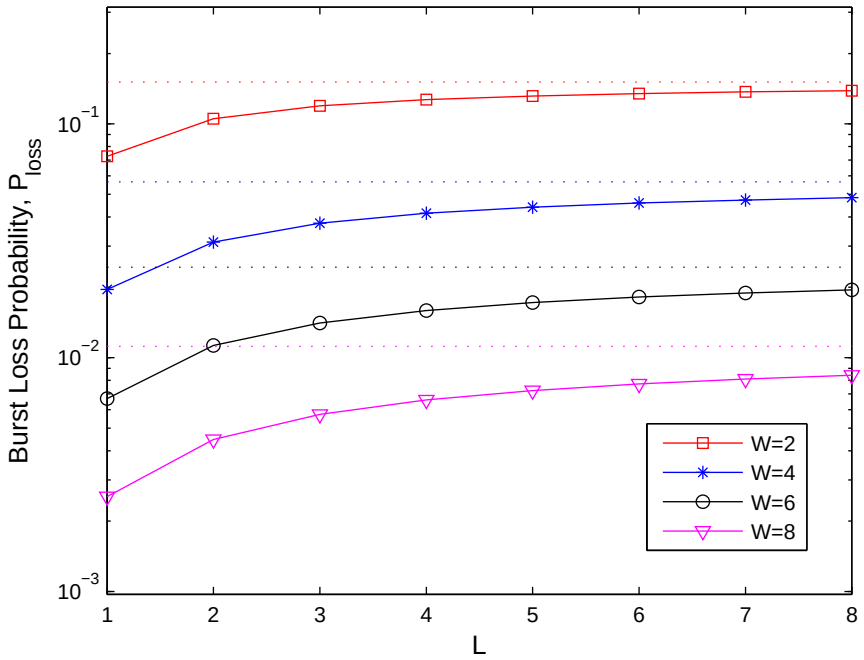

(a) ρ=0.4

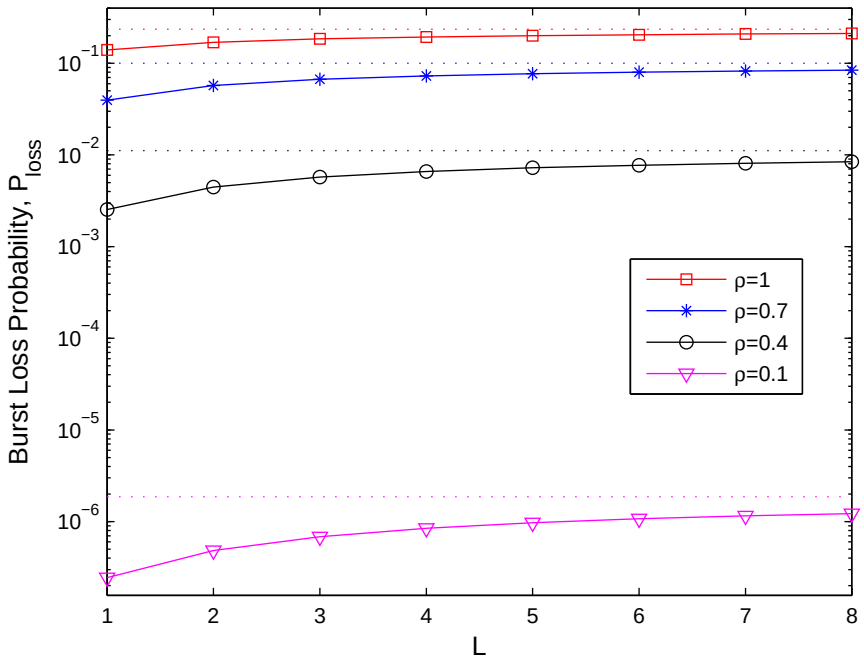

(b) W=8

Figure 3.5: Burst loss probabilities of a classless SOBS node for different values of number of wavelengths, W, and traffic load, ρ

Chapter 4

Burst Blocking Probability Analysis of a Two-Class SOBS Node

In this chapter, we generalize our classless OBS network assumption to a two-class network in which two distinct priority classes namely high priority (h.p.) and low priority (l.p.) exist. Analysis of multi-class SOBS networks where more than two QoS classes are supported are left beyond the scope of this thesis. In the SOBS network model, IP packets belonging to high and low priority traffic are aggregated into separate bursts of equal length at the ingress nodes. BCP signaling and burst scheduling are done according to the preferred QoS scheme. It is assumed that the number of high and low priority BCP arrivals in each slot are independent and Poisson distributed with rates λ_h and λ_l, respectively. For convenience, the same notation with Chapter 3 is preserved for PMF, CDF and CCDF functions of low and high priority BCP arrivals but with superscripts l and h respectively. This notation is replicated for other intermediate definitions when necessary.

4.1 Priority Scheduling Based QoS

In this QoS scheme, synchronous mode of operation is exploited making the schedulers of the optical nodes serve the h.p. bursts first and then let l.p. bursts use the remaining resources just as described in Section 2.3.5. Reservation requests for the upcoming slots are stored for a while and simultaneously evaluated. As a result, l.p. bursts are strictly prevented from blocking the h.p. ones arriving at the same slot.

Since both classes of bursts demand a service for L slots, regardless of the choice of scheduler between these QoS classes, the same transitions will occur between the states of the Markov chain Q presented in Section 3.1. Replacing λ with $\lambda_h + \lambda_l$ in (3.3), T can again be calculated from Table 3.1. Number of states in Q is still given by the number of distinct solutions to (3.1). Prioritization takes its effect while calculating the corresponding drop probabilities from the resulting steady state probability distribution as follows. The loss probability for h.p. bursts is given by

$$P_{loss}^{h} = \frac{\sum_{\bar{\mathbf{s}} \in Q} \pi(\bar{\mathbf{s}}) \mu^{h}(\bar{\mathbf{s}})}{\lambda_h}, \tag{4.1}$$

where

$$\begin{aligned} \mu^{h}(\bar{\mathbf{s}}) &= \sum_{i=s^0+1}^{\infty} q_{(i)}^{h}(i - s^0) \\ &= \lambda_h X_{(s^0-1)}^{h} - s^0 X_{(s^0)}^{h}. \end{aligned} \tag{4.2}$$

(4.1) is the same as (3.8), since h.p. bursts experience the full availability of the resources as in the case of a classless network. On the other hand, the loss probability for l.p. bursts is given by

$$P_{loss}^{l} = \frac{\sum_{\bar{\mathbf{s}} \in Q} \pi(\bar{\mathbf{s}}) \mu^{l}(\bar{\mathbf{s}})}{\lambda_l}, \tag{4.3}$$

where

$$\begin{aligned}\mu^l(\bar{\mathbf{s}}) &= \sum_{k=0}^{s^0-1} q^h_{(k)} \sum_{i=s^0-k+1}^{\infty} q^l_{(i)}[i-(s^0-k)] \\ &\quad + \sum_{k=s^0}^{\infty} q^h_{(k)}\lambda_l \\ &= \sum_{k=0}^{s^0-1} q^h_{(k)}[\lambda_l X^l_{(s^0-k-1)} - (s^0-k)X^l_{(s^0-k)}] \\ &\quad + \lambda_l X^h_{(s^0-1)}.\end{aligned} \tag{4.4}$$

The calculation of loss probability for l.p. bursts is slightly different since it is conditioned on h.p. arrivals in a slot as seen in (4.4). First summation term in this equation corresponds to the h.p. burst arrivals in the interval of $[0, s^0-1]$ for which at least one channel remains for l.p. bursts after h.p. scheduling, whereas the second term corresponds to the number of h.p. burst arrivals in the interval of $[s^0, \infty]$ exceeding all available channels and dropping all l.p. bursts.

Offset based QoS is widely used in the literature for asynchronous OBS networks. In the next section, we introduce and analyze its modified version for SOBS networks.

4.2 Unity-Offset Based QoS

Delaying burst transmission for a predetermined number of slots to ensure a higher probability of finding an available wavelength is one of the candidate QoS mechanisms. With no doubt, setting this QoS offset to L, absolute differentiation between h.p. and l.p. bursts can be guaranteed in an SOBS network. However, this may not be an appropriate strategy for delay sensitive applications. In this study, the QoS offset is confined to a single data slot and its effect is investigated for varying L which is of several data slots. In Section 4.4, we show that this analysis can be used to approximate nonunity offset cases as well. Note that,

the execution of a Reserve Limited Duration based scheduling algorithm such as Horizon is essential in order to maintain offset based QoS.

In Section 3.1, while preparing Table 3.1, identicalness of the bursts from the view point of the optical scheduler is exploited. This property which is valid even in the case of priority scheduling based QoS is no longer applicable to offset based QoS. Offset based differentiation does not rely on explicit choice of the scheduler on bursts. Prioritization is inherent in the superiority of h.p. bursts in reserving wavelengths that will be available one slot after their BCP arrivals. Although burst arrivals are synchronous, BCPs traversing the SOBS network in a separate control channel can be treated as asynchronous. Therefore the scheduler is considered to process them in a random fashion on a first-come-first-serve basis. This randomization could be achieved by taking all permutations of h.p. and l.p. bursts for a given number of arrivals and the corresponding state transitions into consideration. However, that kind of an approach would have a great impact on the scalability of the Markov chain as W and L increase. Therefore, we randomize the processing orders of the h.p. and l.p. bursts by transforming the states of Q such that they are updated on the BCP arrival epochs rather than the data slot epochs. In such a structure, at most one burst being either h.p. or l.p. arrives to the system during state transitions. The probabilities associated with these arrivals are well-adjusted such that the resulting arrival process matches with the Poisson process of the BCP arrivals. If the assumed BCP arrival process were geometrically distributed, then we would safely choose a static burst arrival probability, say α, for each state of the Markov chain. Then $1 - \alpha$ would become the probability for end of arrivals. However, we could only match the first order statistic (i.e., mean value of burst arrivals in a slot) of a Poisson distribution with a single parameter α and this would be a rough approximation. In order to skillfully mimic the Poisson distribution we prefer to use a 2-phase PH type distribution whose Markov chain is shown in Figure 4.1. P^0 is the absorbing state of this 2-phase acyclic PH type distribution

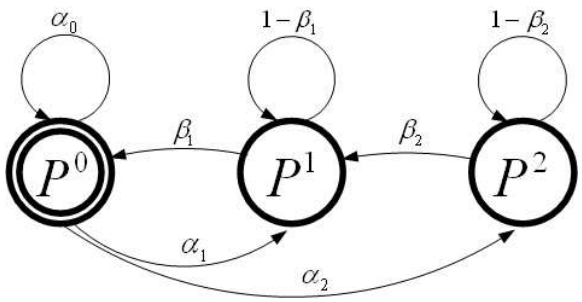

Figure 4.1: Markov chain for 2-phase acyclic PH type distribution

and beginning from this sate all transitions destined to either P^1 or P^2 represents a burst arrival. Transitions to P^0, corresponds to end of arrivals for that slot. Similarly the transition probability α_0 associated with the transition from P^0 to itself gives the probability that no bursts arrive to the core node for that slot.

A similar PH type distribution is elaborately analyzed in [16] to formulate the high-order moment matching problem. In this work, this distribution is used to model the non zero discrete time to absorption, denoted by the random variable M. In other words, M is the random variable for the number of cycles starting from either P^1 or P^2 and ending in P^0. However, in this work M is interpreted as the number of burst arrivals in a slot which is Poisson distributed. Obviously, there is a non-zero probability associated with the case for which no burst arrives. Hence, an additional transition from absorbing state P^0 to itself is defined with a non zero probability of α_0. Propagating this change throughout the analysis performed in [16], we have calculated the transition probabilities of this PH type distribution so that the first two moments of a given Poisson distribution is perfectly matched with a minimized deviation in the third moment. Details of this moment matching process are presented in Appendix A.

We now discuss how this PH type distribution is deployed in the main-stream Markov chain. Q^2 being the Markov chain of this system, $\bar{\mathbf{s}}^2 =$

$(s^0, s^1, \ldots, s^L, s^{L+1}, P^i)$ gives the general description of its states. As compared to the state structure presented in Section 3.1, dimensionality of the state vector $\bar{\mathbf{s}}^2$ is increased by concatenating 3 more substates s^L, s^{L+1} and P^i, where $i = 0, 1, 2$ to $\bar{\mathbf{s}}$, accounting for both the extra QoS offset associated with h.p. bursts and the randomness in the scheduling orders of h.p. and l.p. bursts. In Q^2, probability of an arrival event depends solely on the last substate P^i. Bernoulli trials are then used to generate the priority classes from those arrivals. In offset based QoS, maximum observable horizon by the incoming bursts extends from $L-1$ to L as compared to the classless SOBS due to the unity QoS offset of h.p. bursts. Other than the corresponding state s^L, an extra state s^{L+1} is used whose necessity is explained below together with the scheduling policies applied.

- On a transition to absorbing state P^0, every state s^i transfers its content to the previous state s^{i-1} which means advancing in time. By this evolution, s^{L+1} becomes 0 and s^0 becomes $s^0 + s^1$.

- H.p. bursts are assumed to arrive one slot after their control packets. Hence Q^2 evolves trying to reserve an s^1 wavelength first and then an s^0 wavelength if $s^1 = 0$. If both states are vacant, the burst is blocked. Otherwise s^{L+1} is incremented by one. s^{L+1} is the substate temporarily holding h.p. bursts until a transition to the absorbing state P^0 occurs. This transition represents the end of arrivals for that slot.

- L.p. bursts are assumed to arrive synchronously with their control packets. Hence Q^2 evolves trying to reserve an s^0 wavelength. If $s^0 = 0$, the l.p. burst is blocked. Otherwise s^L is incremented by one. s^L holds both the previously transferred content of s^{L+1} and currently scheduled l.p. bursts until the absorption time.

Based on these guidelines, state transitions are explicitly tabulated in Tables 4.1, 4.3 and 4.2. The parameter set $\{\alpha_0, \alpha_1, \alpha_2, \beta_1, \beta_2\}$ used in these tables are state transition probabilities of the PH type distribution (Figure 4.1) embedded in the Markov chain Q^2 and p_h and p_l are defined as

$$p_h := \text{ P\{ an arriving burst belongs to h.p. class } \} = \frac{\lambda_h}{\lambda_h + \lambda_l},$$
$$p_l := \text{ P\{ an arriving burst belongs to l.p. class } \} = \frac{\lambda_l}{\lambda_h + \lambda_l}.$$

Current State $\bar{\mathbf{s}}^2[n] = (s^0, s^1, \ldots, s^L, 0, P^0)$		
Next State $\bar{\mathbf{s}}^2[n+1] =$	**Transition Condition**	**Transition Probability**
$(s^0 + s^1, s^2, \ldots, s^L, 0, 0, P^0)$		α_0
$(s^0 - 1, s^1, \ldots, s^L + 1, 0, P^1)$	$s^0 > 0$	$\alpha_1 p_l$
$(s^0, s^1, \ldots, s^L, 0, P^1)$	$s^0 = 0$	$\alpha_1 p_l$
$(s^0 - 1, s^1, \ldots, s^L + 1, 0, P^2)$	$s^0 > 0$	$\alpha_2 p_l$
$(s^0, s^1, \ldots, s^L, 0, P^2)$	$s^0 = 0$	$\alpha_2 p_l$
$(s^0, s^1 - 1, \ldots, s^L, 1, P^1)$	$s^1 > 0$	$\alpha_1 p_h$
$(s^0 - 1, s^1, \ldots, s^L, 1, P^1)$	$s^1 = 0, s^0 > 0$	$\alpha_1 p_h$
$(s^0, s^1, \ldots, s^L, 0, P^1)$	$s^1 = 0, s^0 = 0$	$\alpha_1 p_h$
$(s^0, s^1 - 1, \ldots, s^L, 1, P^2)$	$s^1 > 0$	$\alpha_2 p_h$
$(s^0 - 1, s^1, \ldots, s^L, 1, P^2)$	$s^1 = 0, s^0 > 0$	$\alpha_2 p_h$
$(s^0, s^1, \ldots, s^L, 0, P^2)$	$s^1 = 0, s^0 = 0$	$\alpha_2 p_h$

Table 4.1: State transitions from a given state $\bar{\mathbf{s}}^2$, where $P^0 \in \bar{\mathbf{s}}^2$, of the Markov chain Q^2 for unity-offset based differentiation

Total number of states in Q^2 is denoted by N^2. Equation (3.1), with upper limits L, $L+1$ and $L+1$ has to be satisfied for states P^0, P^1 and P^2 respectively. P^0 depicts that no burst has arrived to the optical node from the beginning of a slot. Thus, s^{L+1} holding the number of h.p. bursts arriving in that slot is always zero (Table 4.1) explaining the lower upper limit for P^0. The following equation gives the state count of Q^2. As seen, the number of phases of the chosen PH type distribution approximately comes in a multiplicative factor in the calculation of

Current State $\bar{\mathbf{s}}^2[n] = (s^0, s^1, \ldots, s^L, s^{L+1}, P^1)$		
Next State $\bar{\mathbf{s}}^2[n+1] =$	**Transition Condition**	**Transition Probability**
$(s^0 + s^1, s^2, \ldots, s^L, s^{L+1}, 0, P^0)$		β_1
$(s^0 - 1, s^1, \ldots, s^L + 1, s^{L+1}, P^1)$	$s^0 > 0$	$(1-\beta_1)p_l$
$(s^0, s^1, \ldots, s^L, s^{L+1}, P^1)$	$s^0 = 0$	$(1-\beta_1)p_l$
$(s^0, s^1 - 1, \ldots, s^L, s^{L+1} + 1, P^1)$	$s^1 > 0$	$(1-\beta_1)p_h$
$(s^0 - 1, s^1, \ldots, s^L, s^{L+1} + 1, P^1)$	$s^1 = 0, s^0 > 0$	$(1-\beta_1)p_h$
$(s^0, s^1, \ldots, s^L, s^{L+1}, P^1)$	$s^1 = 0, s^0 = 0$	$(1-\beta_1)p_h$

Table 4.2: State transitions from a given state $\bar{\mathbf{s}}^2$, where $P^1 \in \bar{\mathbf{s}}^2$, of the Markov chain Q^2 for unity-offset based differentiation

N^2:

$$N^2 = \binom{W+L}{W} + \binom{W+L+1}{W} + \binom{W+L+1}{W}. \tag{4.5}$$

Let T^2 be the state transition matrix of Q^2 and $\pi(\bar{\mathbf{s}}^2)$, where $\bar{\mathbf{s}}^2 \in Q^2$, be the steady state probability of a definite state $\bar{\mathbf{s}}^2$. Then blocking probabilities of h.p. and l.p. classes are found using the following notation:

$$\begin{aligned} e(\bar{\mathbf{s}}^2) &:= \text{P\{ an arrival occurs in state } \bar{\mathbf{s}}^2 \text{ \}} \\ \gamma^h(\bar{\mathbf{s}}^2) &:= \text{P\{ an arriving h.p. burst is blocked in state } \bar{\mathbf{s}}^2 \text{ \}} \\ \gamma^l(\bar{\mathbf{s}}^2) &:= \text{P\{ an arriving l.p. burst is blocked in state } \bar{\mathbf{s}}^2 \text{ \}} \end{aligned}$$

$$P^h_{loss} = \frac{\sum_{\bar{\mathbf{s}}^2 \in Q^2} \pi(\bar{\mathbf{s}}^2)\gamma^h(\bar{\mathbf{s}}^2)e(\bar{\mathbf{s}}^2)p_h}{\sum_{\bar{\mathbf{s}}^2 \in Q^2} \pi(\bar{\mathbf{s}}^2)e(\bar{\mathbf{s}}^2)p_h} = \frac{\sum_{\bar{\mathbf{s}}^2 \in Q^2} \pi(\bar{\mathbf{s}}^2)\gamma^h(\bar{\mathbf{s}}^2)e(\bar{\mathbf{s}}^2)}{\sum_{\bar{\mathbf{s}}^2 \in Q^2} \pi(\bar{\mathbf{s}}^2)e(\bar{\mathbf{s}}^2)},$$

where

$$\gamma^h(\bar{\mathbf{s}}^2) = \begin{cases} 1 & \text{if } s^0 + s^1 = 0 \\ 0 & o.w, \end{cases} \tag{4.6}$$

$$e(\bar{\mathbf{s}}^2) = \begin{cases} 1 - \alpha_0 & \text{if } P^0 \in \bar{\mathbf{s}}^2 \\ 1 - \beta_1 & \text{if } P^1 \in \bar{\mathbf{s}}^2 \\ 1 & \text{if } P^2 \in \bar{\mathbf{s}}^2. \end{cases} \tag{4.7}$$

Current State $\bar{\mathbf{s}}^2[n] = (s^0, s^1, \ldots, s^L, s^{L+1}, P^2)$		
Next State $\bar{\mathbf{s}}^2[n+1] =$	**Transition Condition**	**Transition Probability**
$(s^0 - 1, s^1, \ldots, s^L + 1, s^{L+1}, P^2)$	$s^0 > 0$	$(1 - \beta_2)p_l$
$(s^0, s^1, \ldots, s^L, s^{L+1}, P^2)$	$s^0 = 0$	$(1 - \beta_2)p_l$
$(s^0 - 1, s^1, \ldots, s^L + 1, s^{L+1}, P^1)$	$s^0 > 0$	$\beta_2 p_l$
$(s^0, s^1, \ldots, s^L, s^{L+1}, P^1)$	$s^0 = 0$	$\beta_2 p_l$
$(s^0, s^1 - 1, \ldots, s^L, s^{L+1} + 1, P^2)$	$s^1 > 0$	$(1 - \beta_2)p_h$
$(s^0 - 1, s^1, \ldots, s^L, s^{L+1} + 1, P^2)$	$s^1 = 0, s^0 > 0$	$(1 - \beta_2)p_h$
$(s^0, s^1, \ldots, s^L, s^{L+1}, P^2)$	$s^1 = 0, s^0 = 0$	$(1 - \beta_2)p_h$
$(s^0, s^1 - 1, \ldots, s^L, s^{L+1} + 1, P^1)$	$s^1 > 0$	$\beta_2 p_h$
$(s^0 - 1, s^1, \ldots, s^L, s^{L+1} + 1, P^1)$	$s^1 = 0, s^0 > 0$	$\beta_2 p_h$
$(s^0, s^1, \ldots, s^L, s^{L+1}, P^1)$	$s^1 = 0, s^0 = 0$	$\beta_2 p_h$

Table 4.3: State transitions from a given state $\bar{\mathbf{s}}^2$, where $P^2 \in \bar{\mathbf{s}}^2$, of the Markov chain Q^2 for unity-offset based differentiation

$$P_{loss}^{l} = \frac{\sum_{\bar{\mathbf{s}}^2 \in Q^2} \pi(\bar{\mathbf{s}}^2)\gamma^l(\bar{\mathbf{s}}^2)e(\bar{\mathbf{s}}^2)p_l}{\sum_{\bar{\mathbf{s}}^2 \in Q^2} \pi(\bar{\mathbf{s}}^2)e(\bar{\mathbf{s}}^2)p_l} = \frac{\sum_{\bar{\mathbf{s}}^2 \in Q^2} \pi(\bar{\mathbf{s}}^2)\gamma^l(\bar{\mathbf{s}}^2)e(\bar{\mathbf{s}}^2)}{\sum_{\bar{\mathbf{s}}^2 \in Q^2} \pi(\bar{\mathbf{s}}^2)e(\bar{\mathbf{s}}^2)}$$

where

$$\gamma^l(\bar{\mathbf{s}}^2) = \begin{cases} 1 & , \text{ if } s^0 = 0 \\ 0 & , \ o.w \end{cases} \tag{4.8}$$

The two QoS differentiation methods for SOBS networks discussed in Sections 4.1 and 4.2 are combined into a hybrid QoS mechanism in the next section in order to increase the service quality.

Current State $\bar{\mathbf{s}}^3[n] = (s^0, s^1, \ldots, s^{L-1}, s^L)$		
Next State $\bar{\mathbf{s}}^3[n+1] =$	**Transition Condition**	**Transition Probability**
$(s^0 + s^1 - i - j, s^2, \ldots, s^L + j, i)$	$i \leq s^1, j < s^0$	$q^h_{(i)} q^l_{(j)}$
$(s^1 - i, s^2, \ldots, s^L + s^0, i)$	$i \leq s^1, \forall j \geq s^0$	$q^h_{(i)} \sum_{k=s^0}^{\infty} q^l_{(k)} = q^h_{(i)} X^l_{(s^0-1)}$
$(s^0 + s^1 - i - j, s^2, \ldots, s^L + j, i)$	$s^1 < i < s^0 + s^1$ $j < s^0 + s^1 - i$	$q^h_{(i)} q^l_{(j)}$
$(0, s^2, \ldots, s^L + s^0 - (i - s^1), i)$	$s^1 < i < s^0 + s^1$ $\forall j \geq s^0 + s^1 - i$	$q^h_{(i)} \sum_{k=s^0+s^1-i}^{\infty} q^l_{(k)}$ $= q^h_{(i)} X^l_{(s^0+s^1-i-1)}$
$(0, s^2, \ldots, s^L, s^1 + s^0)$	$\forall i \geq s^0 + s^1$	$\sum_{k=s^0+s^1}^{\infty} q^h_{(k)} = X^h_{(s^0+s^1-1)}$

Table 4.4: State transitions from a given state $\bar{\mathbf{s}}^3$ of the Markov chain Q^3 for hybrid priority scheduling with unity-offset based differentiation

4.3 Hybrid Priority Scheduling with Unity-Offset Based QoS

QoS techniques introduced and analyzed in Sections 4.1 and 4.2 can be merged to attain a better QoS capability. In this hybrid scheme, h.p. bursts are allowed to make reservations one slot before their BCP arrivals to the optical node and are further prioritized as these BCPs are selectively serviced in the scheduler. On the other hand, l.p. bursts are assumed to arrive to the optical node without leaving any data slot space between their BCPs and are scheduled always after all h.p. BCPs are processed.

Let Q^3 be the Markov chain constructed to model the behavior of this multiserver system with the aforementioned service policy. Since priority scheduling capability of the optical scheduler is exploited, no randomization in the scheduling order of bursts is needed. Therefore a state $\bar{\mathbf{s}}^3$ of Q^3 can be derived from the presented one in Section 3.1 by only concatenating the sub-state s^L which holds

the number of h.p. bursts scheduled in the previous slot. Note that, Markov chain state transitions for this hybrid model occur from slot-to-slot basis like in the classless case. All possible state transitions from $\bar{\mathbf{s}}^3[n] = (s^0, s^1, \ldots, s^{L-1}, s^L)$ are given in Table 4.3. In Table 4.3, i and j correspond to the total number of h.p. and l.p. reservation requests - or equivalently BCP arrivals - to the optical node on a slot epoch respectively. The state space size of Q^3 is denoted by N^3 and given by the following formula:

$$N^3 = \binom{W+L}{W}. \tag{4.9}$$

Solving Q^3, the burst blocking probabilities of the priority classes are found as follows. Note that, $t := s^0 + s^1$ is used for convenience. The loss probability for h.p. bursts is given by

$$P^h_{loss} = \frac{\sum_{\bar{\mathbf{s}}^3 \in Q^3} \pi(\bar{\mathbf{s}}^3)\mu^h(\bar{\mathbf{s}}^3)}{\lambda_h}, \tag{4.10}$$

where

$$\begin{aligned} \mu^h(\bar{\mathbf{s}}^3) &= \sum_{i=t+1}^{\infty} q^h_{(i)}(i-t) \\ &= \lambda_h X^h_{(t-1)} - t X^h_{(t)}. \end{aligned} \tag{4.11}$$

Equations (4.10) and (4.11) are the same as (4.1) and (4.2), except for the replacement of $t = s^0 + s^1$ by s^0, meaning that not only s^0 wavelengths but also s^1 wavelengths are available for h.p. bursts in this hybrid QoS scheme. The loss probability for l.p. bursts is given by

$$P^l_{loss} = \frac{\sum_{\bar{\mathbf{s}}^3 \in Q^3} \pi(\bar{\mathbf{s}}^3)\mu^l(\bar{\mathbf{s}}^3)}{\lambda_l}, \tag{4.12}$$

where

$$\begin{aligned}\mu^l(\bar{\mathbf{s}}^3) &= \sum_{k=0}^{s^1} q^h_{(k)} \sum_{i=s^0+1}^{\infty} q^l_{(i)}(i-s^0) \\ &\quad + \sum_{k=t}^{\infty} q^h_{(k)} \sum_{i=0}^{\infty} q^l_{(i)} i \\ &\quad + \sum_{k=s^1+1}^{t-1} q^h_{(k)} \sum_{i=t-k+1}^{\infty} q^l_{(i)}[i-(t-k)] \\ &= F^h_{(s^1)}[\lambda_l X^l_{(s^0-1)} - s^0 X^l_{(s^0)}] \\ &\quad + \lambda_l X^h_{(t-1)} \\ &\quad + \sum_{k=s^1+1}^{t-1} q^h_{(k)}[\lambda_l X^l_{(t-k-1)} - (t-k) X^l_{(t-k)}].\end{aligned} \tag{4.13}$$

(4.13) formulates the l.p. loss probability dependence on the h.p. arrivals. The first summation term takes the arriving number of h.p. bursts less than s^1 into account for which no l.p. bursts are dropped. To the contrary, the second summation term considers the case for which more than s^0+s^1 h.p. bursts arrive and all l.p. bursts are dropped. Finally, the third term corresponds to the h.p. burst arrivals exceeding the s^1 wavelengths in number but not using all of the s^0 wavelengths. In this case, the l.p. bursts' resources are partially allocated by the h.p. bursts.

In the next section, numerical solutions of the Markov chain models together with the corresponding simulations for the three QoS schemes discussed in this thesis are presented.

4.4 Numerical Results

In this section, BCP arrival rates of high and low priority bursts are taken equal unless otherwise stated. In Figures 4.2, 4.3 and 4.4, the simulation results for the systems analyzed in Sections 4.1, 4.2 and 4.3 respectively are presented. In these simulations, ratio of the burst length to the slot length, L, is taken as 3.

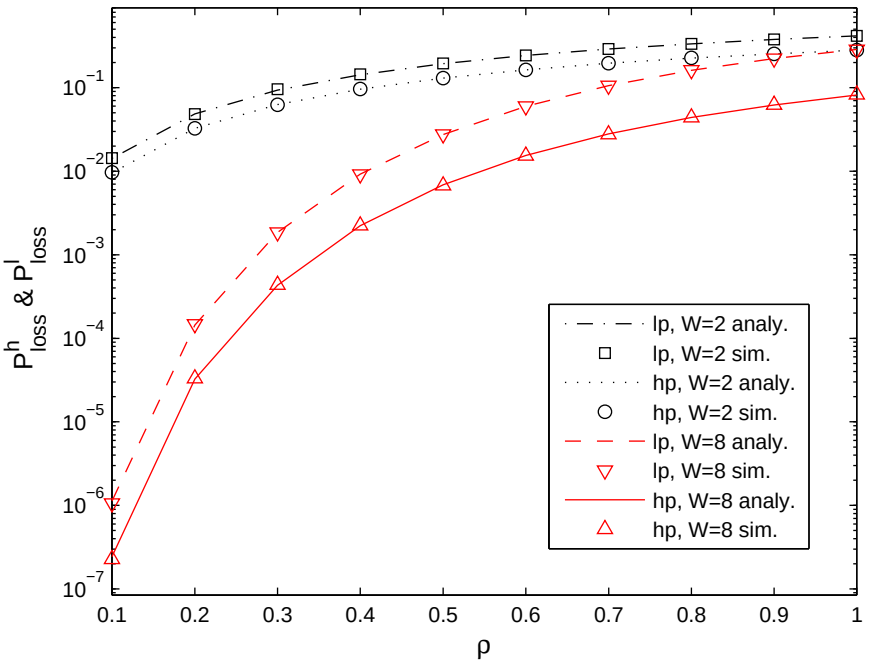

Figure 4.2: Analytical and simulation results for burst loss probabilities of priority scheduling based QoS with $L = 3$

For the analysis of priority scheduling and hybrid priority scheduling with unity-offset based differentiation methods, no further assumptions or approximations are made on top of the presumed models. Therefore, the simulation results do not deviate from the analytically calculated solutions. However, for the unity-offset based differentiation, we approximate the Poisson arrival process with a 2-phase acyclic PH type distribution. Although the first two moments of this arrival process and the PH type distribution are exactly matched, it is seen from Figure 4.3 that as the number of wavelengths W increases, under light traffic loads, ρ, the mismatch in the higher order moments forces the analytical model to estimate a more pessimistic burst loss probability especially for the high priority class.

In Figures 4.5(a) and 4.5(b), QoS performances of the three prioritization methods are compared. We define a QoS metric, Θ, which is the ratio of the low

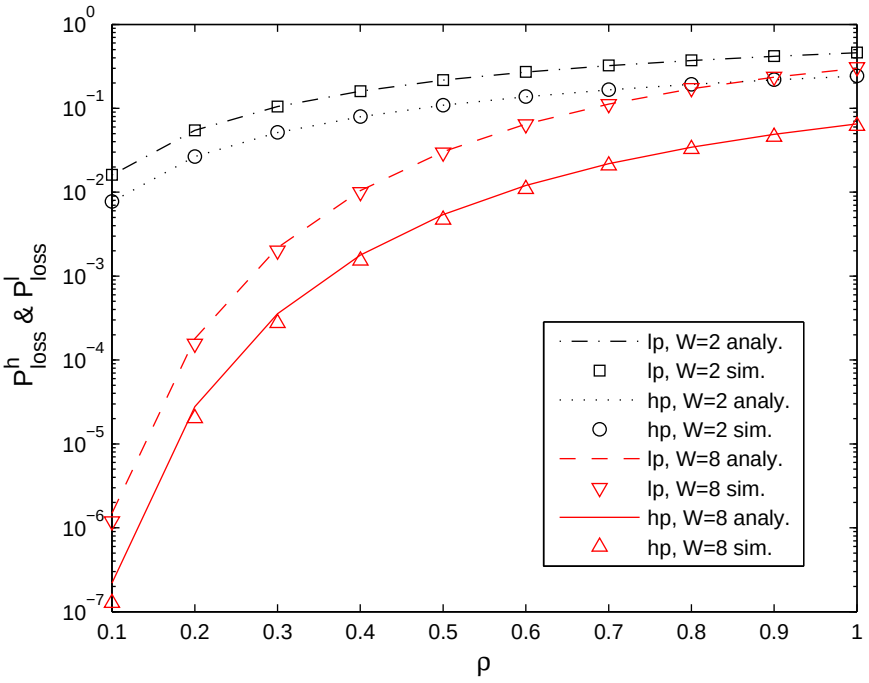

Figure 4.3: Analytical and simulation results for burst loss probabilities of unity-offset based QoS with $L = 3$

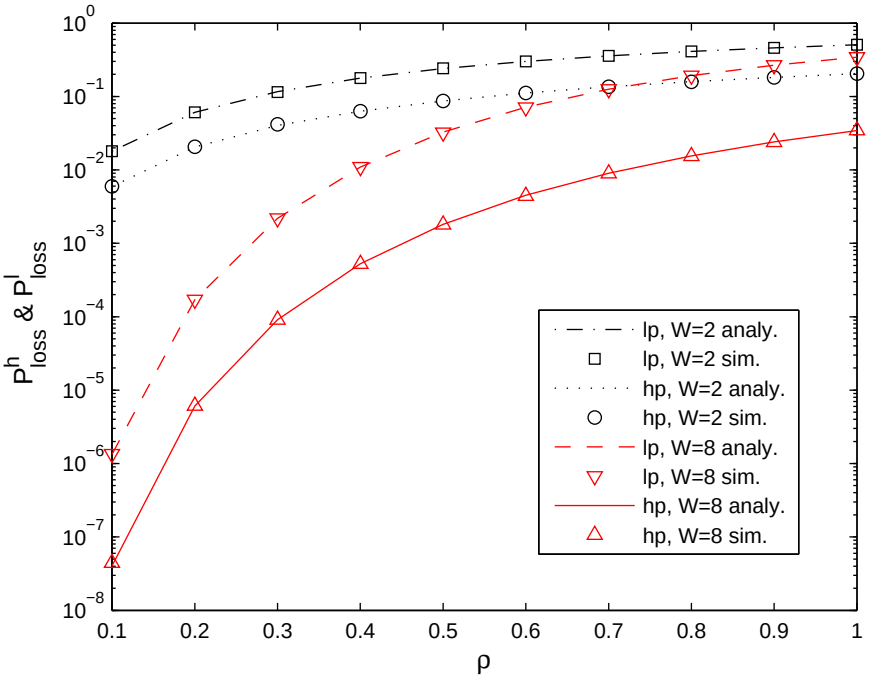

Figure 4.4: Analytical and simulation results for burst loss probabilities of hybrid priority scheduling with unity-offset based QoS with $L = 3$

and high priority class blocking probabilities given by

$$\Theta = \frac{P_{loss}^{l}}{P_{loss}^{h}}.$$

Θ proves to grow with decreasing load, ρ, and increasing total number of wavelengths, W. Among the three proposed QoS schemes, the hybrid mechanism outperforms the others as far as QoS differentiation metric Θ is concerned. These figures also reveal that h.p. bursts benefit from the unity QoS offset slightly more than the preferential treatment in scheduling.

In Figure 4.6, we concentrate on the hybrid QoS scheme. For constant traffic load, ρ, and burst length, L, the effect of varying the proportion of the traffic belonging to the low priority class is plotted. The dashed lines shows the overall burst loss probability, P_{loss}, of the core node which is formulated as

$$P_{loss} = P_{loss}^{l} p_l + P_{loss}^{h}(1 - p_l).$$

P_{loss} remains constant for changing p_l and intersects the high priority and low priority curves at $p_l = 0$ and $p_l = 1$ for all values of W. This behavior is reasonable since when only a single class arrives to the optical node, the QoS advantages and disadvantages disappear. In Figure 4.6, it is evident that, as p_l gets close to one, Θ rapidly increases since high priority bursts become less likely to block each other. On the contrary, low priority bursts begin to collide with each other more frequently as p_l increases.

In Figure 4.7, the response of the hybrid QoS scheme to the variation in burst length to slot length ratio, L, is shown. Independent variable L of the plot is the number of data slots per burst. In the plots, slopes of the burst blocking probability curves bend more steeper near $L = 2$. At that point, full isolation is achieved between the high and low priority classes and the high priority burst blocking probability becomes completely insensitive to the variations in the offered low priority traffic load. When $L = 2$, arriving low priority bursts try to

make reservations for two data slots, which reduce to a single data slot at the next coming slot boundary. By the advantage of their QoS offset, high priority bursts do not differentiate between the wavelengths that is already available or that will be available in one data slot later as far as the available number of wavelengths are concerned. By priority scheduling scheme, they also have the full superiority over the low priority bursts in reserving available channels. Being unaffected by the low priority arrivals in these two cases, high priority bursts are said to be fully isolated from the low priority class when $L = 2$. This isolation gradually decreases as L increases and in the limit where $L \to \infty$, advantage stemming from both the unity QoS offset and priority scheduling becomes negligible. In Figure 4.7, the low priority burst blocking probability seems nearly independent from L, which shows that the decreasing level of QoS and convergence to $M/M/C/C$ loss system cancel out each other as L increases.

In Figure 4.8, it is shown that the burst loss probabilities drop significantly for increasing W under low load conditions. This behavior is in accordance with $M/M/C/C$ loss systems, where the more statistically shared the resources are the smaller the loss probability.

In Figures 4.9(a) and 4.9(b), nonunity QoS offset based differentiation simulation results are given. For increasing QoS offset, T_{QoS}, the h.p. loss probability decreases following approximately a linear regime in the logarithmic scale. When $T_{QoS} = L$, this loss probability line saturates because of the strict isolation attained at this point. From this point on, the l.p. loss probability curve changes its curvature as well, because an l.p. burst can no longer block an h.p. burst.

Generalizing the unity-offset based QoS analysis in Section 4.2 to nonunity offsets requires a dramatic increase in the state space size of the constructed Markov chain. On the other hand, without any further effort, three points on the h.p. loss probability curve can be found as follows. When $T_{QoS} = 0$, the high and low priority classes unify, hence the Markov chain for a classless SOBS

node with a traffic load, ρ, introduced in Chapter 3 can be used to calculate this probability. Similarly, when $T_{QoS} > L$, the h.p. bursts experience a network load consisting of only themselves. Thus, the same Markov chain but with a traffic load of $p_h\rho$ can be used for calculating P^h_{loss}. For $T_{QoS} = 1$, a Markov chain in Section 4.2 is already introduced. A least squares solution can be found for the intermediate probabilities of h.p. class as shown in Figures 4.9(a) and 4.9(b). Assuming this system is work conserving, the l.p. burst loss probability, P^l_{loss}, can be calculated from the overall loss probability, P_{loss} for a classless SOBS node with load ρ as follows:

$$P_{loss} = p_h P^h_{loss} + p_l P^l_{loss}. \tag{4.14}$$

As seen in the figures, the work conservation assumption does not seem to be valid especially for $T_{QoS} > L$. Nevertheless, the l.p. loss probabilities can be computed with an acceptable accuracy in at least the presented cases without requiring significant amount of computation.

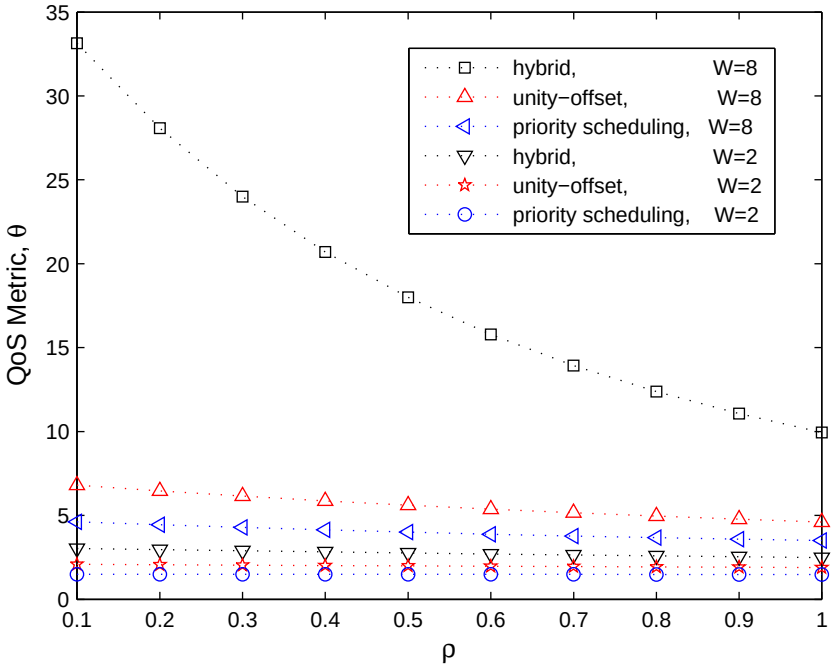

(a) L=3

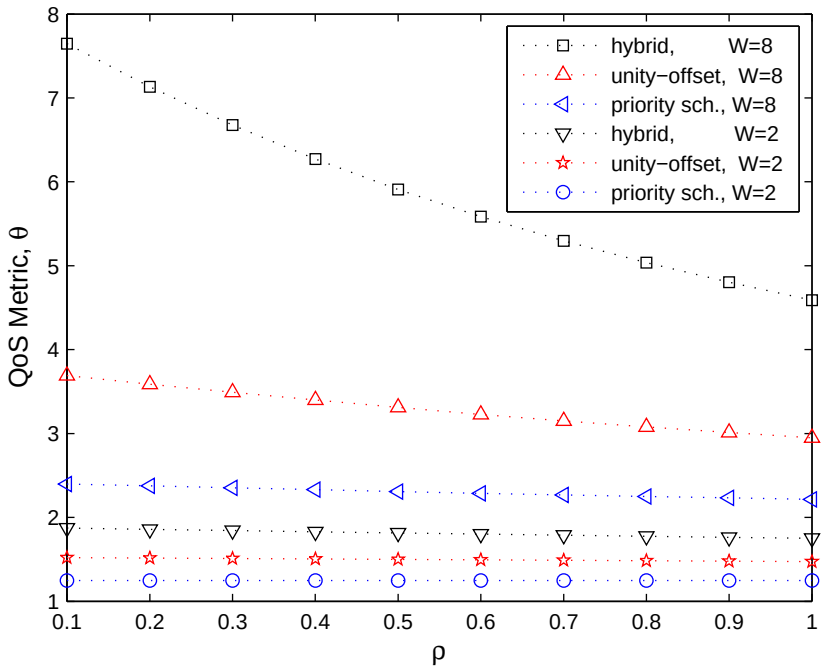

(b) L=5

Figure 4.5: Θ of the three QoS schemes for different values of number of wavelengths, W

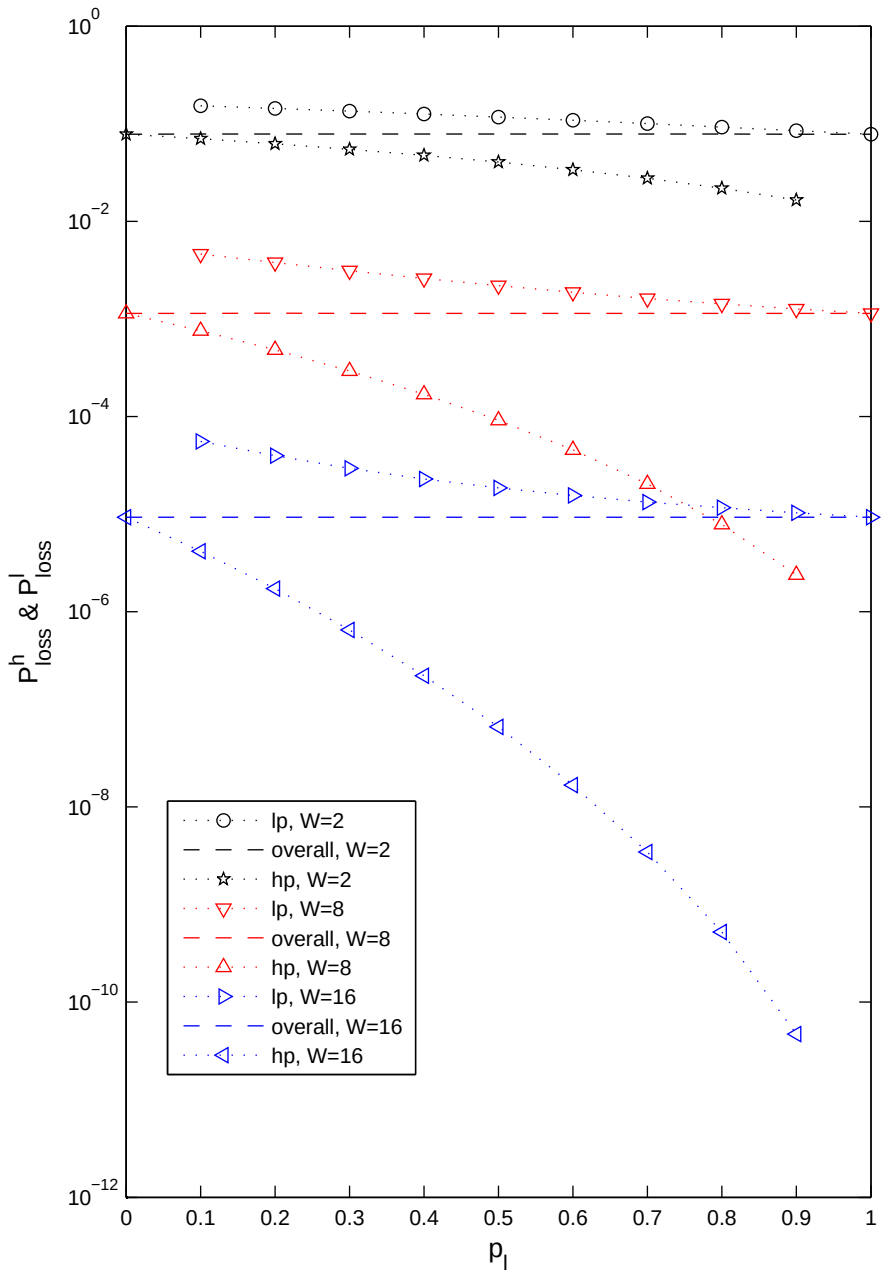

Figure 4.6: Burst loss probabilities of hybrid priority scheduling with unity-offset based QoS scheme with $L = 3$ and $\rho = 0.3$

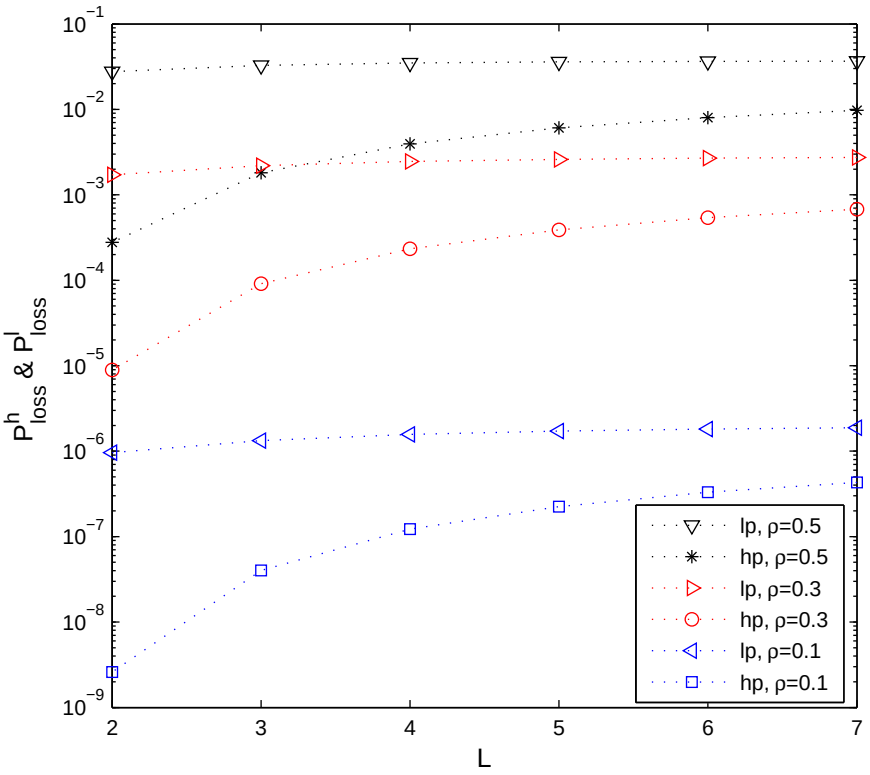

Figure 4.7: Burst loss probabilities of hybrid priority scheduling with unity-offset based QoS scheme with $W = 8$

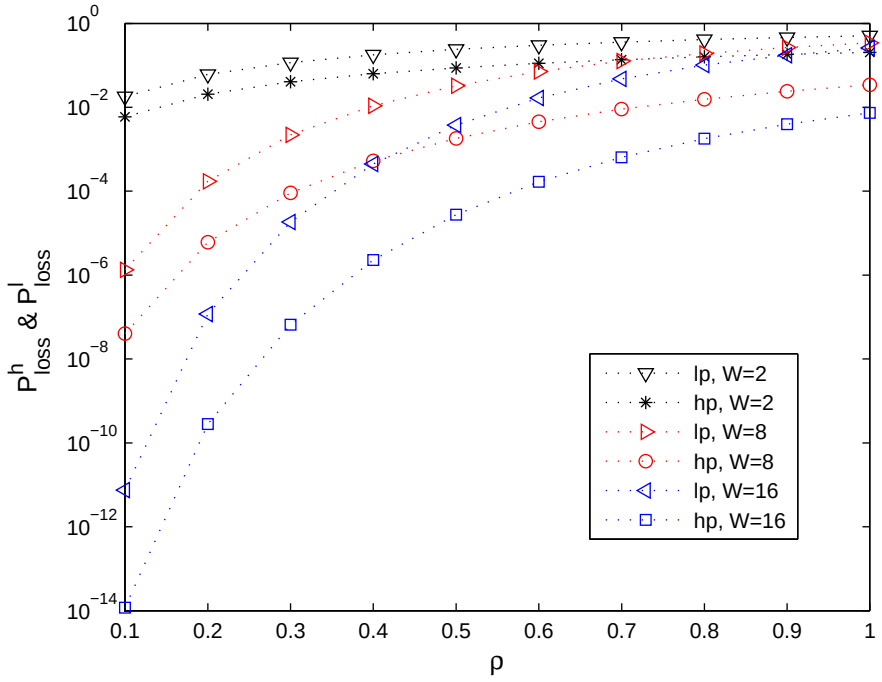

Figure 4.8: Burst loss probabilities of hybrid priority scheduling with unity-offset based QoS scheme with $L = 3$

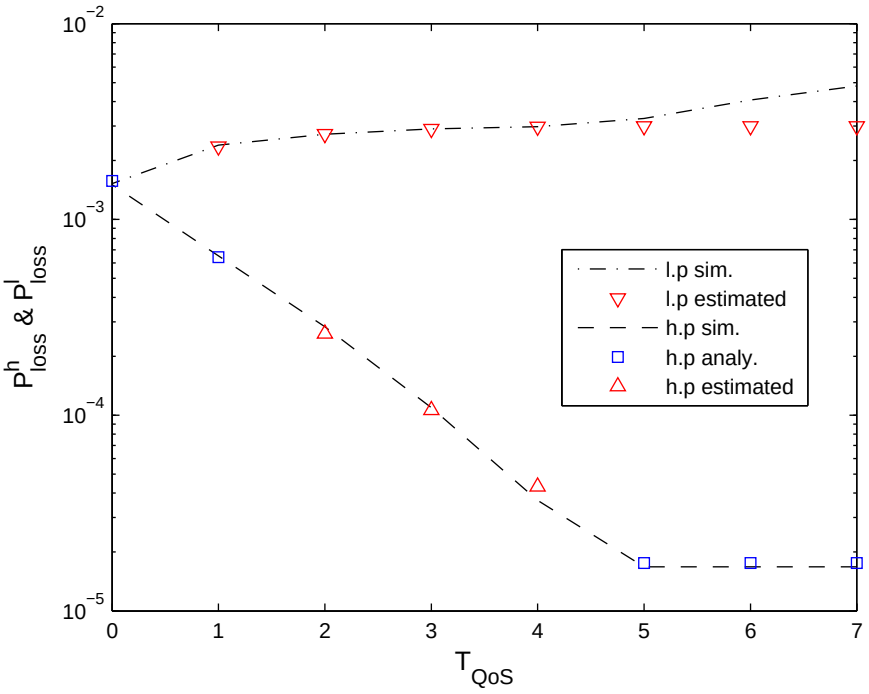

(a) ρ=0.3

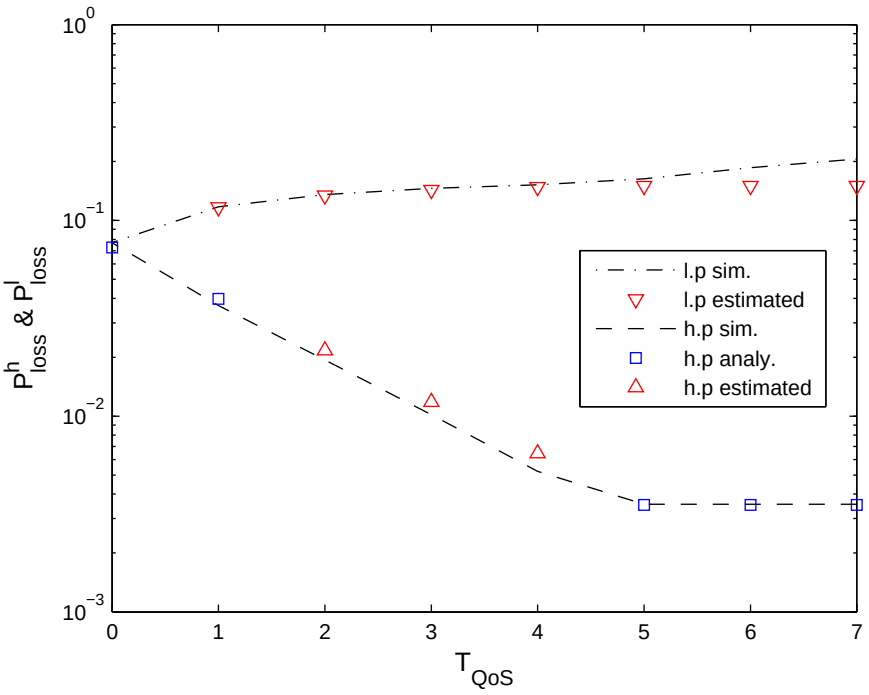

(b) ρ=0.7

Figure 4.9: Burst loss probability estimations of nonunity-offset based QoS scheme for changing QoS offset length, T_{QoS}, with $L = 5$ and $W = 8$

Chapter 5

Conclusion

In this thesis, we develop a Markov chain based framework for performance evaluation of SOBS by which we study the burst blocking probabilities of both a classless and a two-class SOBS core node. We provide with the formulation for burst blocking probability of a classless SOBS node for changing traffic load, ρ, number of wavelengths, W, and burst length, L. Extending this study, we also make an analysis of three QoS schemes appropriate for slotted mode of operation that are priority scheduling, unity-offset and hybrid priority scheduling with unity-offset based differentiation. We validate the accuracy of our framework against simulations.

Results show that, as L increases SOBS asymptotically converges to asynchronous OBS in terms of burst loss probability and this convergence is more rapid for high loss rates where ρ is high and W is low. We also show that, SOBS may provide with a similar performance to the traditional OBS but with a less number of wavelengths and under relatively heavy traffic conditions, increasing the chance of burst switching paradigm to be appraised as the next generation Internet architecture.

Among the three QoS schemes analyzed in this thesis, hybrid priority scheduling with unity-offset based differentiation yields the best isolation between the QoS classes and unity-offset based differentiation ranks the second leaving priority scheduling the last. As W increases and L decreases, a higher isolation level is achieved. By decreasing the proportion of the traffic consisting of high priority bursts, even higher degree in isolation can be reached.

We believe that the proposed framework presented in this thesis can be further extended to analyze some other variations in an SOBS network which are listed as follows.

1. In this thesis, BCP arrivals within a slot are assumed to be Poisson distributed. However, other distributions may be of interest. Proposed Markov chains other than the one for the unity-offset differentiation, use only the PMF, CDF and the CCDF functions of a given arrival process. Hence they offer full flexibility in changing the BCP arrival distribution without sacrificing from precision. However, in the analysis of the unity-offset differentiation, the Poisson distribution is approximated by a discrete phase type distribution. Although moment matching for another distribution can be done according to the formulation given in Appendix A, results would need validation.

2. Fixed length assumption for bursts can be generalized to variable length bursts with a certain statistical distribution.

3. Nonunity QoS offsets, T_{QoS}, for high priority class can also be analyzed with better computational techniques for the solution of large and sparse Markov chain transition matrices.

4. The framework can be extended to the analysis of multi-class networks.

APPENDIX A

Moment Matching for λ

Let $\lambda := \lambda_h + \lambda_l$ be the total BCP arrival rate to the optical node and M be the random variable denoting the number of arrivals generated by the discrete PH type distribution given in Figure 4.1. Then, the probability-generating function of M is written as:

$$\begin{aligned} G_M(z) = E[z^M] &= \alpha_0 + \alpha_1 \frac{\beta_1 z}{1-(1-\beta_1)z} \\ &\quad + \alpha_2 \frac{\beta_2 z}{1-(1-\beta_2)z} \frac{\beta_1 z}{1-(1-\beta_1)z} \end{aligned} \tag{A.1}$$

The first three factorial moments of M are defined as follows.

$$f_1 := \frac{d}{dz} G_M(z)|_{z=1} = E[M] \tag{A.2}$$

$$f_2 := \frac{d^2}{dz^2} G_M(z)|_{z=1} = E[M(M-1)] \tag{A.3}$$

$$f_3 := \frac{d^3}{dz^3} G_M(z)|_{z=1} = E[M(M-1)(M-2)] \tag{A.4}$$

Let Z be the Poisson distributed random variable with rate λ. Then, the following equalities should hold for a perfect moment matching between Z and

M.

$$
\begin{aligned}
f_1 &= E[Z] && \text{(A.5)}\\
&= \lambda \\
f_2 &= E[Z^2 - Z] && \text{(A.6)}\\
&= (\lambda^2 + \lambda) - \lambda \\
&= \lambda^2 \\
f_3 &= E[Z^3 - 3Z^2 + 2Z] && \text{(A.7)}\\
&= (\lambda^3 + 3\lambda^2 + \lambda) - 3(\lambda^2 + \lambda) + 2\lambda \\
&= \lambda^3
\end{aligned}
$$

Since,

$$
\begin{aligned}
&E[(Z - E[Z])^3] = \lambda && \text{(A.8)}\\
&\Rightarrow E[Z^3 - 3Z^2E[Z] + 3ZE[Z]^2 - E[Z]^3] = \lambda \\
&\Rightarrow E[Z^3] - 3(\lambda^2 + \lambda)\lambda + 3\lambda\lambda^2 - \lambda^3 = \lambda \\
&\Rightarrow E[Z^3] = \lambda^3 + 3\lambda^2 + \lambda
\end{aligned}
$$

However, simultaneously solving (A.5), (A.6) and (A.7) is non-feasible for a broad range of λ. Even the second factorial moment formulated by (A.6) requires λ to be lower than a threshold which is found to be 3.72 in Appendix B. Hence, we converted this moment matching problem into a constrained optimization problem as follows.

$$\min_{\alpha_0,\alpha_1,\alpha_2,\beta_1,\beta_2} |f_3 - \lambda^3| \qquad \text{(A.9)}$$

such that,

$$
\begin{aligned}
& f_1 = \lambda \qquad\qquad (A.10)\\
& f_2 = \lambda^2 \\
& \alpha_0 = q_{(0)} \\
& 0 \leq \alpha_1, \alpha_2, \beta_1, \beta_2 \leq 1 \\
& \alpha_0 + \alpha_1 + \alpha_2 = 1
\end{aligned}
$$

Solution to (A.9) and (A.10) in the feasible range of λ gives the parameters $\alpha_0, \alpha_1, \alpha_2, \beta_1$ and β_2 of the PH type distribution shown in Figure 4.1.

APPENDIX B

Upper Bound Calculation for λ

In this section, we calculate the upper bound for λ below which equations (A.2) and (A.3) are guaranteed to be satisfied. They are explicitly solved as follows:

$$f_1 = \frac{\alpha_1\beta_2 + \alpha_2\beta_1 + \alpha_2\beta_2}{\beta_1\beta_2} = \lambda \tag{B.1}$$

$$\begin{aligned} f_2 &= \frac{-2}{\beta_1^2\beta_2^2}(\alpha_1\beta_1\beta_2^2 - \alpha_1\beta_2^2 - \alpha_2\beta_1\beta_2 + \alpha_2\beta_1^2\beta_2 \\ &\quad +\alpha_2\beta_1\beta_2^2 - \alpha_2\beta_1^2 - \alpha_2\beta_2^2) \\ &= \lambda^2, \end{aligned} \tag{B.2}$$

where $\alpha_0 = e^{-\lambda}$ and $\alpha_1 = 1 - \alpha_0 - \alpha_2$ according to (A.10). (B.1) can be solved for α_2 after replacing α_1 by $1 - e^{-\lambda} - \alpha_2$ as follows:

$$\alpha_2 = \lambda\beta_2 - \frac{\beta_2}{\beta_1}(1 - e^{-\lambda}). \tag{B.3}$$

Similarly (B.2) can be simplified after replacing α_1:

$$f_2 = \alpha_2\frac{2(\beta_1 - \beta_1\beta_2 + \beta_2)}{\beta_1\beta_2^2} + (1 - e^{-\lambda})\frac{-2(\beta_1 - 1)}{\beta_1^2} = \lambda^2 \tag{B.4}$$

Substituting α_2 found in (B.3) into (B.4), we end up with the following equality:

$$\lambda^2 - \lambda\frac{2(\beta_1 - \beta_1\beta_2 + \beta_2)}{\beta_1\beta_2} + (1 - e^{-\lambda})\frac{2}{\beta_1\beta_2} = 0. \tag{B.5}$$

(B.5) should be solved for maximum λ for which the following inequality inherited from (B.3) is satisfied:

$$0 \leq \alpha_2 = \lambda\beta_2 - \frac{\beta_2}{\beta_1}(1 - e^{-\lambda}) \leq 1 - e^{-\lambda}. \tag{B.6}$$

The computations of the maximum value of λ for which (B.5) can be solved such that (B.6) is satisfied do not have a simple closed form solution. By making use of numerical methods, an upper bound on λ for which the first two moments of the PH type distribution matches with the Poisson distribution is obtained to be 3.72358161 for a precision of 10^{-8}. Figures B.1-B.4 depicts the regions of β_1 and β_2, where (B.5) and (B.6) are both feasible for a given λ. As seen from the plots, for $\lambda > 3.72$, regions for equality (B.5) and inequality (B.6) do not intersect anymore meaning that exact matching of the first two moments is not possible beyond this point.

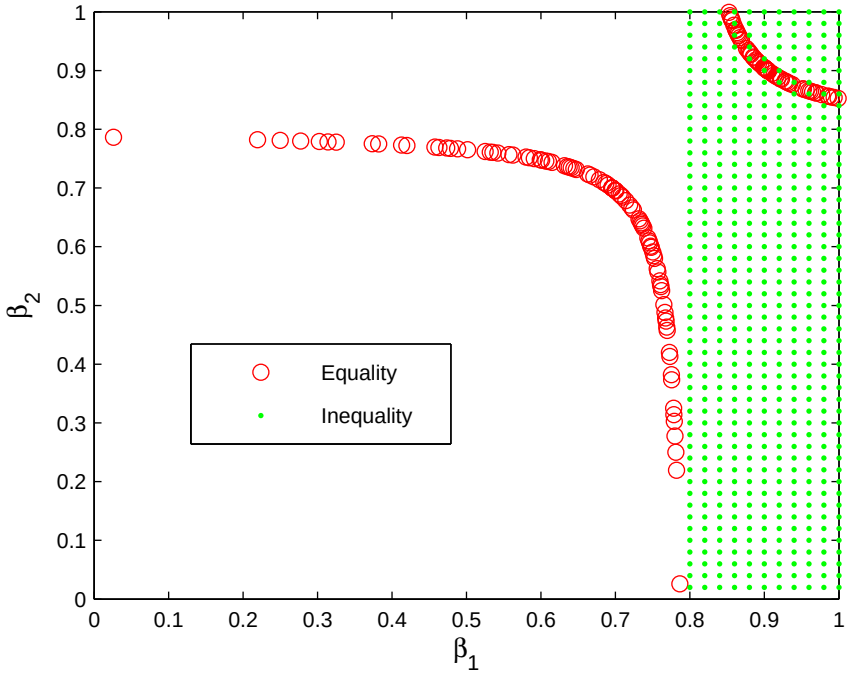

Figure B.1: Feasible regions of (B.5) and (B.6) for $\lambda = 0.5$

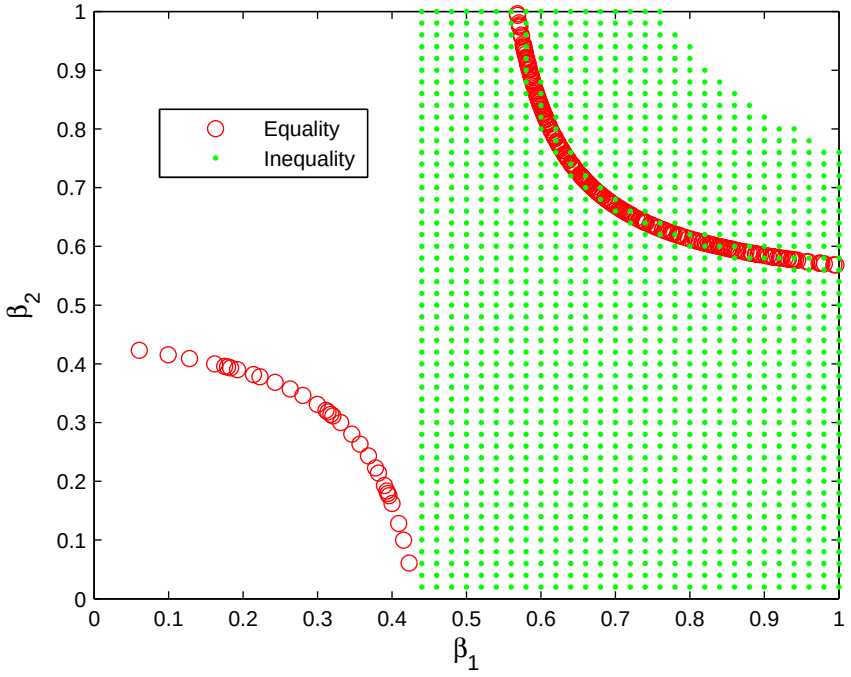

Figure B.2: Feasible regions of (B.5) and (B.6) for $\lambda = 2$

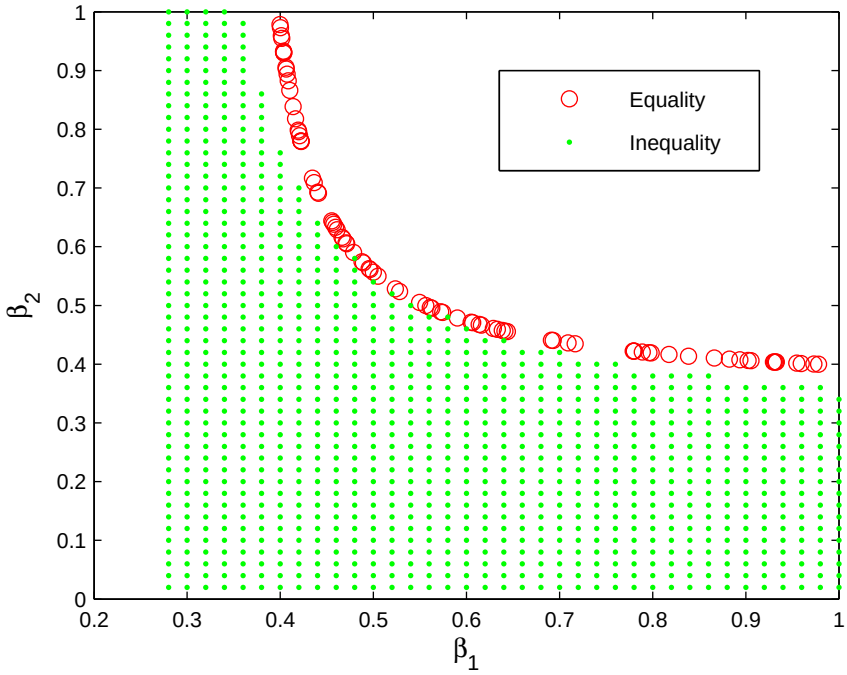

Figure B.3: Feasible regions of (B.5) and (B.6) for $\lambda = 3.72$

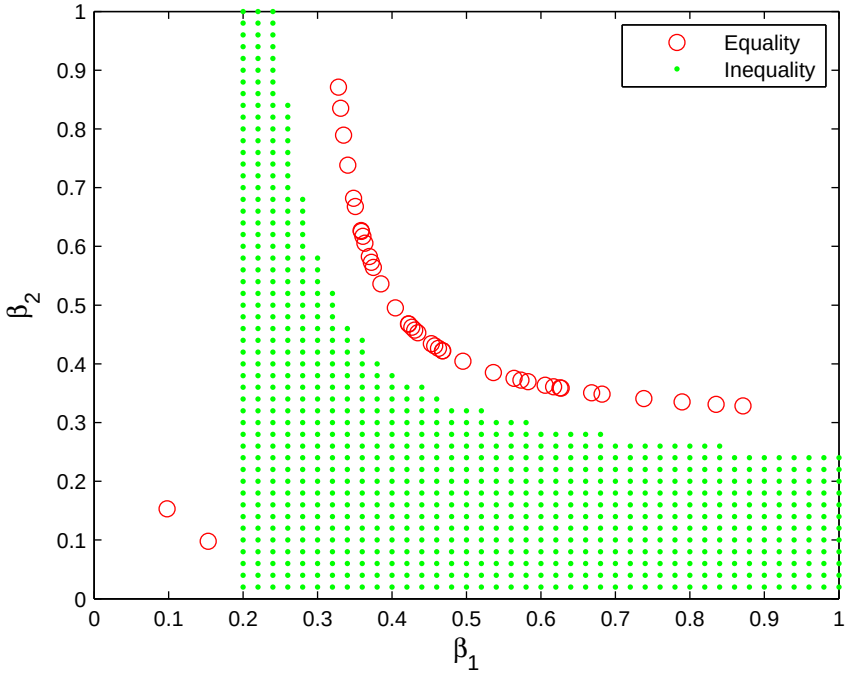

Figure B.4: Feasible regions of (B.5) and (B.6) for $\lambda = 5$

Bibliography

[1] C. Qiao and M. Yoo, "Optical burst switching (OBS) - a new paradigm for an optical Internet," *Journal of High Speed Networks (JHSN)*, vol. 8, no. 1, pp. 69–84, 1999.

[2] S. Verma, H. Chaskar, and R. Ravikanth, "Optical burst switching: a viable solution for terabit IP backbone," *IEEE Network Magazine*, vol. 14, no. 6, pp. 48–53, 2000.

[3] Y. Chen, C. Qiao, and X. Yu, "Optical burst switching: A new area in optical networking research," *IEEE Network Magazine*, vol. 18, no. 3, pp. 16–23, 2004.

[4] M. Yoo and C. Qiao, "Just-enough-time (JET): a high speed protocol for bursty traffic in optical networks," *Proceedings of the Third SPIE Conference on All-Optical Communication Systems*, vol. 3230, no. 1, pp. 79–90, 1997.

[5] K. Lee and V. Li, "A wavelength convertible optical network," *Journal of Lightwave Technology*, vol. 11, pp. 962–970, 1993.

[6] R. A. Barry and P. Humblet, "Models of blocking probability in all-optical networks with and without wavelength changers," *IEEE Journal on Selected Areas in Communications*, vol. 14, pp. 858–867, 1996.

[7] C. Gauger, "Optimized combination of converter pools and FDL buffers for contention resolution in optical burst switching," *Photonic Network Communications*, vol. 8, no. 2, pp. 139–148, 2004.

[8] A. Zalesky, H. L. Vu, Z. Rosberg, E. W. M. Wong, and M. Zukerman, "Stabilizing deflection routing in optical burst switched networks," *IEEE Journal on Selected Areas in Communications*, vol. 25, no. 6, pp. 3–19, 2007.

[9] N. Akar, E. Karasan, and K. Dogan, "Wavelength converter sharing in asynchronousoptical packet/burst switching: An exact blocking analysis for Markovian arrivals," *IEEE Journal on Selected Areas in Communications*, vol. 24, no. 12, pp. 69–80, 2006.

[10] S. Yao, S. J. B. Yoo, B. Mukherjee, and S. Dixit, "All-optical packet switching for metropolitan area networks: opportunities and challenges," *IEEE Communications Magazine*, vol. 39, no. 3, pp. 142–148, 2001.

[11] F. Farahmand, V. M. Vokkarane, and J. P. Jue, "Practical priority contention resolution for slotted optical burst switching networks," *Proceedings of the First International Workshop on Optical Burst Switching (WOBS)*, 2003.

[12] A. Rugsachart, *Time synchronized optical burst switching.* PhD thesis, University of Pittsburgh, August 2007.

[13] Z. Zhang, L. Liu, and Y. Yang, "Slotted optical burst switching (SOBS) networks," *Proceedings of the Fifth IEEE International Symposium on Network Computing and Applications (NCA '06)*, pp. 111–117, 2006.

[14] J. Li, C. Qiao, J. Xu, and D. Xu, "Maximizing throughput for optical burst switching networks," *Transactions on Networking*, vol. 15, no. 5, pp. 1163–1176, 2007.

[15] M. Yoo, C. Qiao, and S. Dixit, "QoS performance of optical burst switching in IP-over-WDM networks," *IEEE Journal on Selected Areas in Communications*, vol. 18, no. 10, pp. 2062–2071, 2000.

[16] M. Telek and A. Heindl, "Matching moments for acyclic discrete and continous phase-type distributions of second order," *International Journal of Simulation Systems, Science & Technology*, vol. 3, no. 3–4, pp. 47–57, 2002.

[17] R. Tucker and W. Zhong, "Photonic packet switching: an overview," *IEICE Transactions on Communications*, vol. E82-B, pp. 254–264, 1999.

[18] I. Widjaja, "Performance analysis of burst admission-control protocols," *IEE Proceedings-Communications,*, vol. 142, no. 1, pp. 7–14, 1995.

[19] A. Ge, F. Callegati, and L. Tamil, "On optical burst switching and self-similar traffic," *IEEE Communications Letters,*, vol. 4, no. 3, pp. 98–100, 2000.

[20] V. M. Vokkarane, K. Haridoss, and J. P. Jue, "Threshold-based burst assembly policies for QoS support in optical burst-switched networks," *Optical Networking and Communications (OptiComm 2002)*, vol. 4874, no. 1, pp. 125–136, 2002.

[21] X. Yu, Y. Chen, and C. Qiao, "Study of traffic statistics of assembled burst traffic in optical burst-switched networks," *Optical Networking and Communications (OptiComm 2002)*, vol. 4874, no. 1, pp. 149–159, 2002.

[22] Y. Xiong, M. Vandenhoute, and H. Cankaya, "Control architecture in optical burst-switched WDM networks," *IEEE Journal on Selected Areas in Communications*, vol. 18, no. 10, pp. 1838–1851, 2000.

[23] K. Dolzer, C. Gauger, J. Spth, and S. Bodamer, "Evaluation of reservation mechanisms for optical burst switching," *International Journal of Electronics and Communications (AE)*, vol. 55, no. 1, pp. 18–26, 2001.

[24] I. Baldine, G. Rouskas, H. Perros, and D. Stevenson, "Jumpstart: a just-in-time signaling architecture for WDM burst-switched networks," *IEEE Communications Magazine*, vol. 40, no. 2, pp. 82–89, 2002.

[25] J. Y. Wei and R. I. McFarland, "Just-in-time signaling for WDM optical burst switching networks," *Journal of Lightwave Technology*, vol. 18, no. 12, pp. 2019–2037, 2000.

[26] G. Hudek and D. Muder, "Signaling analysis for a multi-switch all-optical network," *IEEE International Conference on Communications (ICC 95)*, vol. 2, pp. 1206–1210, 1995.

[27] J. Y. Wei, J. L. Pastor, R. S. Ramamurthy, and Y. Tsai, "Just-in-time optical burst switching for multiwavelength networks," *Broadband communications: Convergence of Network Technologies*, vol. 159, pp. 339–352, 1999.

[28] C. Qiao and M. Yoo, "Choices, features and issues in optical burst switching (OBS)," *Optical Networking Magazine*, vol. 1, no. 2, pp. 37–44, 2000.

[29] J. S. Turner, "Terabit burst switching," *Journal of High Speed Networks (JHSN)*, vol. 8, no. 1, pp. 3–16, 1999.

[30] Y. Xiong, M. Vandenhoute, and H. C. Cankaya, "Design and analysis of optical burst-switched networks," *All-Optical Networking 1999: Architecture, Control, and Management Issues*, vol. 3843, no. 1, pp. 112–119, 1999.

[31] J. Xu, C. Qiao, J. Li, and G. Xu, "Efficient channel scheduling algorithms in optical burst switched networks," *Proceedings of the Twenty-Second Annual Joint Conference of the IEEE Computer and Communications Societies (INFOCOM 2003)*, vol. 3, pp. 2268–2278, 2003.

[32] J. Teng and G. N. Rouskas, "A comparison of the JIT, JET, and Horizon wavelength reservation schemes on a single OBS node," *Proceedings of the First International Workshop on Optical Burst Switching (WOBS)*, 2003.

[33] Z. Rosberg, H. L. Vu, M. Zukerman, and J. White, "Performance analyses of optical burst-switching networks," *IEEE Journal on Selected Areas in Communications*, vol. 21, no. 7, pp. 1187–1197, 2003.

[34] C. M. Gauger, "Performance of converter pools for contention resolution in optical burst switching," *Optical Networking and Communications (OptiComm 2002)*, vol. 4874, no. 1, pp. 109–117, 2002.

[35] C. M. Gauger, "Dimensioning of FDL buffers for optical burst switching nodes," *Proceedings of the Fifth IFIP Optical Network Design and Modeling Conference*, 2002.

[36] D. Hunter, M. Chia, and I. Andonovic, "Buffering in optical packet switches," *Journal of Lightwave Technology*, vol. 16, no. 12, pp. 2081–2094, 1998.

[37] X. Wang, H. Morikawa, and T. Aoyama, "Deflection routing protocol for burst-switching WDM mesh networks," *Terabit Optical Networking: Architecture, Control, and Management Issues*, vol. 4213, no. 1, pp. 242–252, 2000.

[38] Y. Chen, H. Wu, D. Xu, and C. Qiao, "Performance analysis of optical burst switched node with deflection routing," *IEEE International Conference on Communications (ICC '03)*, vol. 2, pp. 1355–1359, 2003.

[39] X. Wang, H. Morikawa, and T. Aoyama, "A deflection routing protocol for optical bursts in WDM networks," *Proceedings of the Fifth Optoelectronics and Communications Conference (OECC)*, pp. 94–95, 2000.

[40] C.-F. Hsu, T.-L. Liu, and N.-F. Huang, "Performance analysis of deflection routing in optical burst-switched networks," *Proceedings of the Twenty-First Annual Joint Conference of the IEEE Computer and Communications Societies (INFOCOM 2002)*, vol. 1, pp. 66–73, 2002.

[41] A. Detti, V. Eramo, and M. Listanti, "Performance evaluation of a new technique for IP support in a WDM optical network: Optical composite burst switching (OCBS)," *Journal of Lightwave Technology*, vol. 20, p. 154, 2003.

[42] V. Vokkarane, J. Jue, and S. Sitaraman, "Burst segmentation: an approach for reducing packet loss in optical burst switched networks," *IEEE International Conference on Communications (ICC 2002)*, vol. 5, pp. 2673–2677, 2002.

[43] V. Vokkarane, Q. Zhang, J. Jue, and B. Chen, "Generalized burst assembly and scheduling techniques for QoS support in optical burst-switched networks," *IEEE Global Telecommunications Conference (GLOBECOM '02)*, vol. 3, pp. 2747–2751, 2002.

[44] M. Yoo and C. Qiao, "Supporting multiple classes of services in IP over WDM networks," *IEEE Global Telecommunications Conference (GLOBECOM '99)*, vol. 1B, pp. 1023–1027, 1999.

[45] N. Barakat and E. Sargent, "Analytical modeling of offset-induced priority in multiclass OBS networks," *IEEE Transactions on Communications*, vol. 53, no. 8, pp. 1343–1352, 2005.

[46] K. Dolzer and C. Gauger, "On burst assembly in optical burst switching networks - a performance evaluation of Just-Enough-Time," *Proceedings of the 17th International Teletraffic Congress*, pp. 149–161, 2001.

[47] Y. Chen, M. Hamdi, and D. Tsang, "Proportional QoS over OBS networks," *IEEE Global Telecommunications Conference (GLOBECOM '01)*, vol. 3, pp. 1510–1514, 2001.

[48] T. L. Battestilli, "Optical burst switching: A survey," *Technical Report TR-2002-10, North Carolina State University*, 2003.

[49] M. Yang, S. Zheng, and D. Verchere, "A QoS supporting scheduling algorithm for optical burst switching DWDM networks," *IEEE Global Telecommunications Conference (GLOBECOM '01)*, vol. 1, pp. 86–91, 2001.

[50] J. Ramamirtham and J. Turner, "Time sliced optical burst switching," *Proceedings of the Twenty-Second Annual Joint Conference of the IEEE Computer and Communications Societies (INFOCOM 2003)*, vol. 3, pp. 2030–2038, 2003.

[51] J. Elmirghani and H. Mouftah, "All-optical wavelength conversion: technologies and applications in DWDM networks," *IEEE Communications Magazine*, vol. 38, no. 3, pp. 86–92, 2000.

[52] A. Rugsachart and R. A. Thompson, "An analysis of time-synchronized optical burst switching," *Workshop on High Performance Switching and Routing*, 2006.

[53] A. Rugsachart and R. A. Thompson., "Optimal timeslot size for synchronous optical burst switching," *Proceedings of the Fourth International Conference on Broadband Communications, Networks and Systems (BROADNETS 2007)*, 2007.

[54] S. Yao, B. Mukherjee, and S. Dixit, "Advances in photonic packet switching: an overview," *IEEE Communications Magazine*, vol. 38, no. 2, pp. 84–94, 2000.

[55] J. Cheyns, E. Van Breusegem, C. Develder, A. Ackaert, M. Pickavet, and P. Demeester, "Performance improvement of an internally blocking optical packet/burst switch," *IEEE International Conference on Communications (ICC '03)*, vol. 2, pp. 1304–1308, 2003.

[56] LAPACK++ is a library for high performance linear algebra computations, http://sourceforge.net/projects/lapackpp, 2008.